



## Hf isotope evidence for variable slab input and crustal addition in basalts and andesites of the Taupo Volcanic Zone, New Zealand



Tod E. Waight <sup>a,\*</sup>, Valentin R. Troll <sup>b</sup>, John A. Gamble <sup>c,d</sup>, Richard C. Price <sup>e</sup>, Jane P. Chadwick <sup>f</sup>

<sup>a</sup> Department of Geosciences and Natural Resource Management (Geology Section), Copenhagen University, Øster Voldgade 10, 1350 Copenhagen K, Denmark

<sup>b</sup> Department of Earth Sciences, Section for Mineralogy, Petrology & Tectonics, Uppsala University, Villavägen 16, 75236 Uppsala, Sweden

<sup>c</sup> School of Geography, Environment and Earth Sciences, Victoria University of Wellington, P.O. Box 600, New Zealand

<sup>d</sup> School of Biological, Earth and Environmental Sciences, University College Cork, Cork, Ireland

<sup>e</sup> Faculty of Science and Engineering, University of Waikato, Private Bag 3105, Hamilton, New Zealand

<sup>f</sup> Science Gallery, Trinity College Dublin, Pearse Street, Dublin 2, Ireland

### ARTICLE INFO

#### Article history:

Received 22 December 2016

Accepted 9 April 2017

Available online 18 April 2017

#### Keywords:

Taupo Volcanic Zone, New Zealand

Hf and Nd isotopes

AFC processes

Source addition

Basalt

Andesite

### ABSTRACT

Crustal contamination complicates the identification of primary mantle-derived magma compositions in continental arcs. However, when crustal processes and components are well characterised, it is possible to extrapolate through continental arc magma compositional arrays towards the Hf and Nd isotope compositions of uncontaminated primary magmas. This is because of the similar behaviour of Hf and Nd during fractional crystallisation and mantle melting, and the subsequent limited variation in Hf/Nd in mantle-derived magmas and in many crustal lithologies, resulting in linear contamination trends for Hf-Nd isotopes. Here we present new Hf isotope data for a selection of volcanic rocks and crustal lithologies from the Taupo Volcanic Zone (TVZ), New Zealand and propose that the scatter in Hf-Nd isotopes indicates heterogeneity in the parental magmas prior to interactions with crustal lithologies. The observed variations likely represent variability in primary magma compositions as a result of different degrees of sediment addition at the slab-wedge interface. Coupled variations in isotopic composition, LILE/HFSE ratios (e.g. Rb/Zr and Ba/La) and SiO<sub>2</sub> also clearly indicate that shallower level crustal interactions have occurred. Andesites from Ruapehu Volcano have more consistent parental magma compositions, and require greater amounts of a source sediment contribution. Notably, the compositions of older Ruapehu lavas can be modelled by interactions between mantle-derived magmas and lower crustal granulites, whereas younger lavas have probably interacted more with mid- to shallow crustal meta-sedimentary greywacke-argillite lithologies of the Permian to Cretaceous composite Torlesse Terrane. Hf-Nd isotopic compositions of meta-igneous granulite xenoliths from Mt. Ruapehu are consistent with previous interpretations that they are derived from oceanic crust that underlies the Torlesse meta-sediments. The results indicate that interactions with sediments at both the slab-wedge interface and in the lithosphere must be considered when evaluating trace element and isotopic variations in continental arcs.

© 2017 Elsevier B.V. All rights reserved.

### 1. Introduction

Subduction zones are the major site of interaction between the Earth's mantle and crust, but the timing and location of these interactions are complex and controversial. Two general models are referred to here: 1) *source addition* where sedimentary material and fluids derived from the subducted slab are added to the mantle source in the asthenosphere; and 2) *crustal addition* where material from the overriding plate is incorporated into the magma as it transects the lithosphere. Traditional petrological and isotope approaches are able to identify if crustal contributions have occurred, but discriminating between

when and where they occurred is difficult. Source addition is often recognised as having a fundamental influence on the geochemistry of oceanic arcs (e.g., Davidson et al., 2005; Duggen et al., 2008; Elliott et al., 1997; Handley et al., 2007, 2011; Pearce et al., 1999; Plank and Langmuir, 1993; Todd et al., 2011), although crustal addition is now increasingly recognised as also being important in these environments (e.g., Beard et al., 2014, 2015; Davidson and Wilson, 2011). Evidence for source addition in continental arcs will usually be overprinted by magma mixing, crustal interactions and fractional crystallisation during transit through the lithosphere and generation of more evolved compositions (e.g., Chadwick et al., 2013; Davidson et al., 2005; Kent et al., 2010; Price et al., 2012; Reubi and Blundy, 2009; Troll et al., 2013). Moreover, discriminating between source and crustal addition in continental arcs is further complicated by the broadly similar compositions of subducted sediment and continental crust.

\* Corresponding author.

E-mail address: [todw@ign.ku.dk](mailto:todw@ign.ku.dk) (T.E. Waight).

In this context, combined Hf and Nd isotope studies have proven invaluable in understanding the role of various components (e.g., slab, fluids, sediments, mantle wedge) in oceanic arc magmatism, particularly in the SW Pacific region (e.g., Pearce et al., 1999, 2007; Todd et al., 2011; Woodhead et al., 2012). This study expands on those of Todd et al. (2010, 2011) who demonstrated that variations in Hf and Nd isotope composition oblique to the mantle array in the oceanic Kermadec arc, north of New Zealand, can be attributed to varying contributions from sediments and sediment-melts to variable ambient mantle wedge compositions during source addition. Similarly variable contributions likely also occur to the south under the continental Taupo Volcanic Zone (TVZ) of the North Island of New Zealand. Understanding magma genesis here is complicated by interactions with continental lithosphere which potentially mask important compositional variations in primary magma compositions (Carter et al., 1996). However, the similar geochemical behaviour of Hf and Nd during fractionation and contamination processes is a potentially useful tool for ‘seeing through’ crustal contamination processes to identify the parental compositions of primary magmas prior to interaction with the lithosphere. We therefore present the first Hf isotope data for basalts, andesites and crustal components from the TVZ.

Variations in isotopic compositions due to interactions between magmas and crust can be modelled using bulk mixing (e.g., Langmuir et al., 1978) or combined assimilation and fractional crystallisation (AFC - De Paolo, 1981). The curvature of mixing and AFC trajectories on isotope diagrams is controlled by the relative concentrations of the elements of interest ( $K$ ) in the respective end-members A and B, e.g., in the case of Hf and Nd isotopes

$$K = \frac{(\text{Hf/Nd})_A}{(\text{Hf/Nd})_B}$$

Values of  $K < 1$  or  $> 1$  will result in curved mixing trends, whereas  $K$  values close to 1 will result in linear mixing trends. Hf and Nd behave similarly during most geological processes and as a consequence there is limited variation in Hf/Nd in most mantle-derived magmas and crustal components typically involved during crustal contamination. The resultant  $K$  values are close to 1 and thus mixing models approach straight lines. To put this in perspective, compilations of global mid-ocean ridge basalts (MORB) show a variation in Hf/Nd of  $0.24 \pm 0.03$  (1SD;  $n = 685$ ) (Arevalo and McDonough, 2010) whereas estimated average upper continental crust has Hf/Nd = 0.20 (Rudnick and Gao, 2003). Examining the TVZ in more detail, there is limited variation in Hf/Nd in end-member components likely to be involved in magmatism. For example, arc and back arc rocks from the oceanic Tonga-Kermadec arc, Lau Basin and Havre Trough have an average Hf/Nd of  $0.20 \pm 0.04$  (1SD;  $n = 111$ ) (data compiled from Pearce et al. (2007), Todd et al. (2011), and Woodhead et al. (2001)), Ruapehu andesites have Hf/Nd =  $0.26 \pm 0.04$  (1SD;  $n = 193$ ) (Price et al., 2012) and a compilation of 355 TVZ rhyolites by Deering et al. (2008) gives Hf/Nd =  $0.25 \pm 0.07$  (1SD) which is in good agreement with an average of  $0.23 \pm 0.01$  for 25 post-25.4 ka rhyolite eruptions from Taupo investigated by Barker et al. (2015). In comparison, TVZ meta-sedimentary basement samples have Hf/Nd of  $0.21 \pm 0.04$  (1SD;  $n = 21$ ; this study and Price et al., 2015).

In AFC models the curvature of modelled contamination trends is also affected by the respective elemental partition coefficients in the fractionating assemblage. A large difference in partition coefficients will result in rapidly changing elemental ratios in the evolving melt component producing an increasing curvature for AFC trajectories on isotope diagrams. Hf and Nd have similar partition coefficients in minerals that dominate crystallisation assemblages in mafic-intermediate magmas (olivine, orthopyroxene, clinopyroxene, plagioclase, Fe-oxides). For example, bulk partition coefficients calculated using the fractionating assemblages for TVZ basalts of Gamble et al. (1990) and the partition coefficients of Claeson and Meurer (2004) range from

0.03 to 0.09 for Hf and from 0.04 to 0.05 for Nd. Crystallisation of minor amounts of amphibole or apatite in more intermediate compositions will have an insignificant effect on these bulk partition coefficients. Thus, fractional crystallisation will not result in major changes in Hf/Nd, and AFC trends for crustal contamination will approach straight lines on isotope variation diagrams, similar to those defined by simple mixing. This makes it possible to see through crustal addition and extrapolate back towards the likely compositions of parental magmas prior to interaction with the lithosphere. Our results show that there must have been heterogeneity in the Hf and Nd isotopic composition of TVZ primary magmas, likely reflecting variations in sediment source addition similar to those observed to the north in the Kermadec Arc (e.g. Todd et al., 2011).

### 1.1. Geological background

The TVZ represents the southern continuation of the oceanic Tonga-Kermadec island arc and Lau Basin-Havre Trough back arc system into New Zealand and is a zone of back-arc rifting and continental magmatism. It results from oblique subduction of oceanic lithosphere of the Pacific Plate beneath the Australian Plate, with subduction rates on the order of 50 mm/yr (e.g., Cole, 1990) (Fig. 1). Rifting and extension (ca. 8 mm/yr, Darby and Meertens, 1995) result in high geothermal gradients and abundant geothermal and volcanic activity (e.g., Bibby et al., 1995; Hochstein et al., 1993; Stern, 1987; Stern et al., 2010). Over the past 2 Ma, volcanic activity in the TVZ has been dominated by rhyolites, typically as caldera-forming eruptions producing large-volume ignimbrites (e.g. Wilson and Rowland, 2016; Wilson et al., 1995). Basaltic magmas in the TVZ are volumetrically rare (<1%) (Gamble et al., 1990, 1993a), nevertheless potentially significant in terms of understanding primary magma compositions.

Basalts occur mostly as small scoria cones and tuff rings located along fault zones in the central region of the TVZ (Hiess et al., 2007). They are typically porphyritic (5–20% phenocrysts), comprising olivine, plagioclase and pyroxene (dominantly clinopyroxene). The basalts are high alumina basalts and have typical subduction signatures with depletions in the high field strength elements (HFSE), and enrichments in the large ion lithophile elements (LILE), and they have the most primitive isotopic signatures in the TVZ. However, compared to oceanic basalts from the Kermadec Arc and Havre Trough, the TVZ basalts are typically more enriched in LILE and show a spread in isotopic signatures from values similar to those observed in the Kermadec Arc towards more radiogenic Sr and less radiogenic Nd isotopic compositions. Gamble et al. (1993a) argued that this reflects crustal addition through combined assimilation and fractional crystallisation (AFC-style) processes. In contrast, Rooney and Deering (2013) have suggested that variations in LILE abundances in the TVZ basalts reflect variable degrees of source addition and crustal addition is disregarded. Our new data allow an evaluation of these differing interpretations.

Modern andesitic volcanism in the TVZ occurs in the composite White Island and Ruapehu and Tongariro stratovolcanoes at the northern and southern end of the TVZ, respectively. Andesitic activity was more abundant earlier in the history of the TVZ, but most of these older systems are now buried beneath later rhyolitic eruptives (Browne et al., 1992; Chambeffet et al., 2014; Wilson et al., 1995). The andesitic volcanoes are currently the most active eruptive systems in the TVZ with multiple, although volumetrically minor, eruptions over the last century (e.g., Gamble et al., 1999). The eruptive products (lavas, scoria and ash) are typically highly porphyritic, dominated by phenocrysts of complexly zoned plagioclase, orthopyroxene and clinopyroxene with rare olivine and amphibole. Erupted compositions are dominantly basaltic andesite to andesite but vary from rare basaltic compositions through to dacites (e.g., Cole et al., 2000; Hobden et al., 2002; Price et al., 2012; Waight et al., 1999).

Understanding crustal addition in the TVZ requires assessment of the basement geology of the TVZ, which is dominated by Permian to

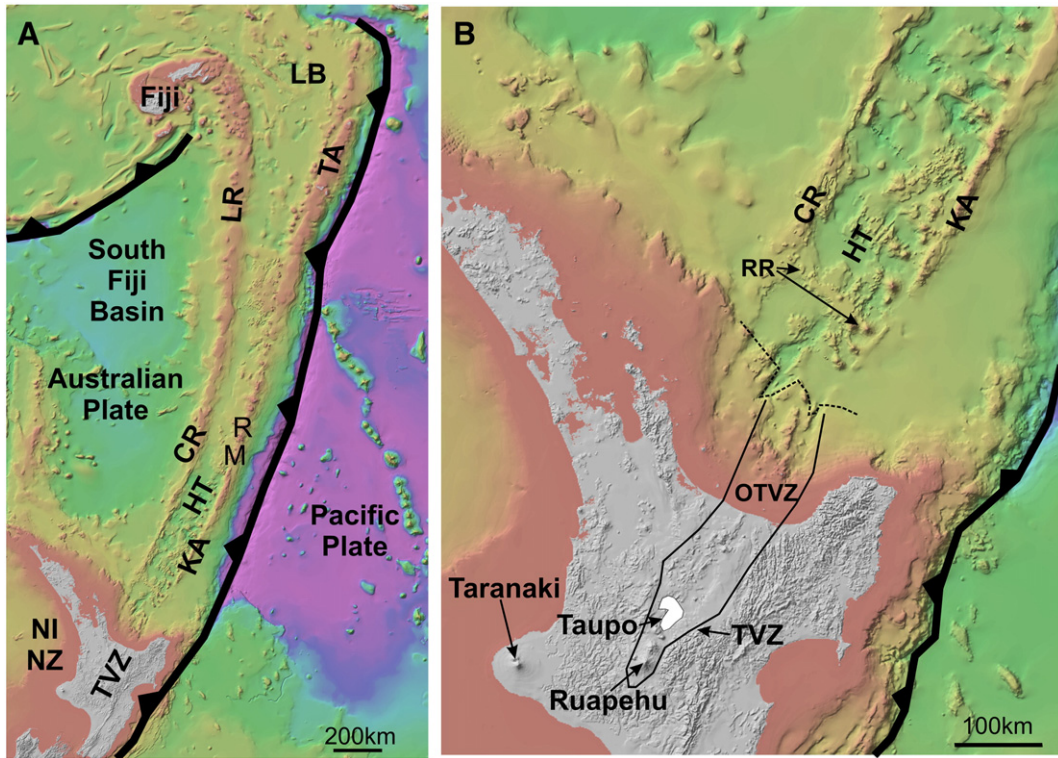


**Fig. 1.** A) Overview of SW Pacific region showing location of the Australia-Pacific Plate boundary and associated subduction features, including the Lau Basin (LB), Tonga Arc (TA), Kermadec Arc (KA), Havre Trough (HT), Colville Ridge (CR), Lau Ridge (LR), North Island, New Zealand (NINZ), Taupo Volcanic Zone (TVZ), Raoul Volcano (R), and Macauley Volcano (M) (modified from Todd et al. (2011)). B) Detail of TVZ and southern KAHT, OTVZ = offshore TVZ, RR = Rumble V Ridge, dashed line = approximate continent-ocean transition (see Gamble et al. (1993a, 1993b) for more details). Background bathymetry is from NIWA ([www.niwa.co.nz/our-science/oceans/bathymetry](http://www.niwa.co.nz/our-science/oceans/bathymetry)).

early Cretaceous submarine fan turbidite greywacke-argillites of the Torlesse Composite Terrane (Kaweka and Pahau Terranes) and their metamorphic equivalents (Adams and Maas, 2004; Mortimer, 2004; Price et al., 2015) (Fig. 2). To the west of the TVZ, the basement changes to the more volcanogenic meta-sediments of the Waipapa Terrane (Fig. 2) however these are not considered to play a significant role in TVZ magmatism. In the south of the TVZ granulitic xenoliths are found in Tongariro and Ruapehu andesites that may represent residues from

melting of fragments of oceanic crust on which the Torlesse sediments were deposited (Graham and Hackett, 1987; Graham et al., 1990; Price et al., 2005).

To the north of the TVZ, the subduction system transforms into the oceanic island arc system of the Kermadec arc and associated Havre Trough back arc (e.g., Barker et al., 2013; Gamble et al., 1993b, 1994, 1996; Macpherson et al., 1998; Smith and Price, 2006; Smith et al., 2003, 2010; Wysoczanski et al., 2010). Todd et al. (2010, 2011) characterised the compositional variability of components involved in oceanic arc magmatism and in this study we assume that these same components are involved in the TVZ. Ambient mantle wedge compositions have been defined on the basis of back arc basin samples that show minimal evidence for addition of slab components and display a limited spread in Hf-Nd isotopic compositions, indicative of both relatively enriched and depleted components. Todd et al. (2010, 2011) also demonstrated a spread in Hf and Nd isotope compositions in the volcanic rocks of the Kermadec Arc and Havre Trough away from ambient mantle wedge that can be explained by variable addition of a slab-derived component (comprising subducted sediments and altered oceanic crust). Addition of even minor amounts (<1%) of these components to the mantle wedge shifts Hf-Nd isotope compositions over the mantle reference line (i.e. towards more radiogenic Hf at a given Nd isotope ratio - see Fig. 6 in Todd et al., 2010, 2011).

## 2. Samples and methods

We present the first Hf isotope data for a suite of representative volcanic samples from the TVZ and the surrounding basement. Major and trace elements and Sr-Nd isotope data for most of these samples have been presented previously (see Table 1 for details). The data include ten geographically spread basalt samples from the TVZ previously described by Gamble et al. (1993a). A suite of andesitic type samples from Ruapehu stratovolcano are investigated including a basalt and

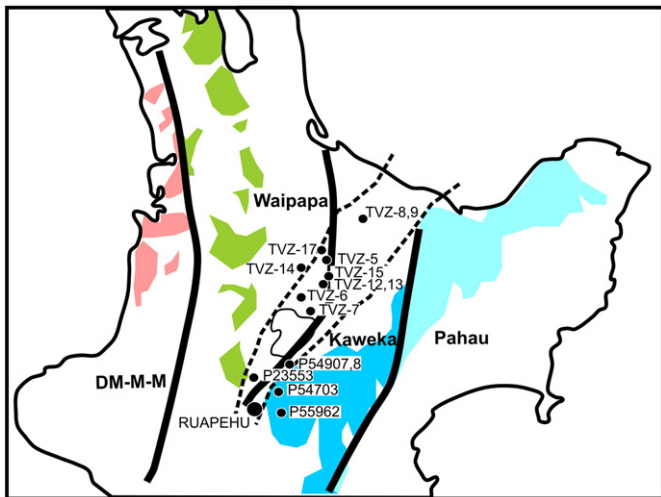


**Fig. 2.** Sample location map. Shaded regions represent outcrops of basement lithologies. The approximate boundaries of the main basement terranes (Dun Mountain-Maitai-Murihiku Terranes (DM-M-M), Waipapa Terrane and the composite Torlesse Terrane (comprising the Kaweka and Pahau Terranes) are shown as solid lines. It is likely that these terrane boundaries dip to the west. The TVZ is represented by the dotted lines. (Modified from Price et al. (2015).)

**Table 1**

Sr, Nd and Hf isotope data for basalts, andesites, and crustal lithologies from the Taupo Volcanic Zone. Previously published Sr and Nd isotope data (in italics) from a) Gamble et al. (1993a) b) Price et al. (2012), c) Waight et al. (1999) and d) Price et al. (2005). All errors are 2SD absolute in the final decimal places (data from Price et al. (2012) have typical in-run precisions (2SE) of  $\pm 0.000020$  and  $\pm 0.000012$  for Sr and Nd respectively).  $\epsilon$ Nd and  $\epsilon$ Hf are calculated using the CHUR values of Bouvier et al. (2008) (0.512630 and 0.282785 respectively).

Sample no.	Description	$^{87}\text{Sr}/^{86}\text{Sr}$	$^{143}\text{Nd}/^{144}\text{Nd}$	$\epsilon\text{Nd}$	$^{176}\text{Hf}/^{177}\text{Hf}$	$\epsilon\text{Hf}$
<i>TVZ basalts</i>						
TVZ-12	Tatua	$0.704122 \pm 20^a$	$0.512879 \pm 5^a$	+4.86	$0.282999 \pm 20$	+7.56
TVZ-14	Ongaroto	$0.704347 \pm 10^a$	$0.512870 \pm 4^a$	+4.68	$0.282887 \pm 7$	+3.59
TVZ-15	Kakuki	$0.703878 \pm 11^a$	$0.512913 \pm 5^a$	+5.52	$0.283003 \pm 7$	+7.72
TVZ-13	Tatua	$0.704076 \pm 20^a$	$0.512880 \pm 5^a$	+4.88	$0.283025 \pm 8$	+8.47
TVZ-5	Atiamuri	$0.704546 \pm 13^a$	$0.512831 \pm 5^a$	+3.92	$0.282916 \pm 8$	+4.63
TVZ-6	Ben Lomond	$0.704300 \pm 12^a$	$0.512860 \pm 5^a$	+4.49	$0.282960 \pm 5$	+6.17
TVZ-7	Trig 9474	$0.704549 \pm 13^a$	$0.512845 \pm 6^a$	+4.19	$0.282931 \pm 25$	+5.16
TVZ-8	Rotokawau E	$0.705064 \pm 19^a$	$0.512791 \pm 5^a$	+3.14	$0.282919 \pm 11$	+4.73
TVZ-9	Rotokawau W	$0.705002 \pm 10^a$	$0.512798 \pm 5^a$	+3.28	$0.282872 \pm 8$	+3.08
TVZ-17	Harry Johnson	$0.704717 \pm 14^a$	$0.512797 \pm 7^a$	+3.26	$0.282910 \pm 6$	+4.43
<i>Ruapehu</i>						
R04/04	Ruapehu Basalt	$0.704746^b$	$0.512931^b$	+5.87	$0.283112 \pm 8$	+11.56
T6-27	Te Herenga	$0.705024^b$	$0.512888^b$	+5.03	$0.283089 \pm 17$	+10.74
T6-15	Te Herenga	$0.704904^b$	$0.512926^b$	+5.77	$0.283109 \pm 6$	+11.47
R95/20	Post-Te Herenga	$0.704966^b$	$0.512808^b$	+3.47	$0.283003 \pm 8$	+7.71
R95/16	Post-Te Herenga	$0.705805^{b,c}$	$0.512686^{b,c}$	+1.09	$0.282914 \pm 5$	+4.56
R97/81	Post-Te Herenga	$0.705302 \pm 24^b$	$0.512744 \pm 12^b$	+2.22	$0.282957 \pm 6$	+6.08
<i>Sediments</i>						
P23553	Waipapa	$0.707322 \pm 11$	$0.512427 \pm 9$	-3.96	$0.282666 \pm 4$	-4.20
P54703	Torlesse	$0.712460 \pm 14$	$0.512385 \pm 14$	-4.77	$0.282666 \pm 4$	-4.19
P55908	Torlesse	$0.710808 \pm 14$	$0.512372 \pm 13$	-5.04	$0.282635 \pm 6$	-5.30
P55962	Torlesse	$0.709510 \pm 14$	$0.512422 \pm 12$	-4.06	$0.282669 \pm 5$	-4.10
P55907	Torlesse	$0.708389 \pm 14$	$0.512384 \pm 16$	-4.80	$0.282629 \pm 5$	-5.52
<i>Xenoliths</i>						
R97/92x1	Meta-igneous	$0.706234 \pm 16^d$	$0.512809 \pm 6^d$	+3.49	$0.282910 \pm 8$	+4.43
R97/92x2	Meta-igneous	$0.707370 \pm 17$	$0.512828 \pm 9$	+3.86	$0.282922 \pm 6$	+4.85
R97/87x1	Meta-igneous	$0.706106 \pm 18$	$0.512948 \pm 9$	+6.20	$0.283034 \pm 8$	+8.82
R97/75b	Meta-igneous	$0.706861 \pm 18$	$0.512900 \pm 8$	+5.27	$0.282912 \pm 6$	+4.48
R97/50b	Meta-igneous	$0.707971 \pm 15$	$0.512948 \pm 8$	+6.20	$0.282979 \pm 6$	+6.87
R97/104x	Meta-sedimentary	$0.707225 \pm 14^d$	$0.512429 \pm 6^d$	-3.92	$0.282680 \pm 6$	-3.72

andesites from the older Te Herenga Formation (250–180 ka) and younger post-Te Herenga Formation eruptives (see Price et al., 2012). While previous work (e.g. Graham and Hackett, 1987; Price et al., 2012) considered the Ruapehu basalt part of the post-Te Herenga eruptives, recent Ar-Ar dating (Conway et al., 2016) indicates that it is part of the Te Herenga Formation and it is treated as such here. In order to characterise potential crustal components, we analysed four samples of Torlesse Composite Terrane sedimentary rocks and a sample of the Waipapa Terrane as referred to in the New Zealand GNS Science PETLAB database. Andesites from Ruapehu volcano invariably contain a suite of mm-cm sized xenoliths that vary from meta-igneous granulites to metasedimentary schists or gneisses and a selection of these are also analysed. Sample locations are shown in Fig. 2.

New trace element analyses were obtained for the TVZ basalt samples and meta-sedimentary basement samples by flux fusion ICPMS at ACTLabs using the 4LITHORES protocol. The full data set of major and trace element analyses is presented in electronic Appendix A. All Hf isotopes compositions were determined using MC-ICP-MS on ca. 100 mg of powder dissolved using flux fusion techniques and analysed using protocols described by Ulfbeck et al. (2003). Full procedural blanks were ca. 50 pg Hf and are negligible compared to the amounts of Hf analysed (150+ ng). Replicate analyses of standards over the period of analysis gave JMC475 =  $^{176}\text{Hf}/^{177}\text{Hf} = 0.282144 \pm 14$  (2 SD, n = 5); all data have been corrected to be equivalent to JMC475  $^{176}\text{Hf}/^{177}\text{Hf} = 0.28216$ . Strontium and neodymium isotope analyses for the TVZ rhyolite and meta-sedimentary basement samples were determined by TIMS in Copenhagen using methods similar to those described by Scott et al. (2014). NIST SRM987 yielded an  $^{87}\text{Sr}/^{86}\text{Sr}$  ratio of  $0.710235 \pm 17$  (2 SD, n = 4) and the internal JM Nd standard (JM) yielded a  $^{143}\text{Nd}/^{144}\text{Nd}$  ratio of  $0.511099 \pm 6$  (2 SD, n = 3) during this study, in good agreement with laboratory averages. Strontium and neodymium isotopes for the Ruapehu xenoliths were determined

at La Trobe University, Melbourne using methods described in Waight et al. (1999) and Price et al. (2012). NIST SRM987 yielded an  $^{87}\text{Sr}/^{86}\text{Sr}$  ratio of  $0.710270 \pm 7$  (n = 2) and La Jolla Nd gave a  $^{143}\text{Nd}/^{144}\text{Nd}$  ratio of  $0.511841 \pm 3$  (n = 3) during this study; Nd isotope values have been adjusted to a  $^{143}\text{Nd}/^{144}\text{Nd}$  ratio of 0.51186. Total procedure blanks for Sr and Nd were <300 pg in both labs and negligible compared to sample sizes analysed. Estimates of reproducibility of Sr and Nd isotope analyses are based on replicates of standard analyses in the Copenhagen lab (SRM987  $^{87}\text{Sr}/^{86}\text{Sr} = 0.710240 \pm 17$  (2 SD, n = 23) and JNDI  $^{143}\text{Nd}/^{144}\text{Nd} = 0.512094 \pm 14$  (2 SD, n = 12); Scott et al., 2014).

### 3. Results

Major and trace element data for the analysed samples are presented in Appendix A and isotope data are presented in Table 1. There is a relatively wide spread in Sr and Nd isotope compositions for TVZ volcanics (Fig. 3), which cover a comprehensive spectrum of observed lithologies in the TVZ (e.g., Gamble et al., 1993a; Price et al., 2005, 2012). The most mafic compositions of the TVZ basalts have relatively radiogenic Sr and unradiogenic Nd compared to typical offshore Kermadec Arc volcanoes. This is likely to be due to interaction with crustal materials (Gamble et al., 1990, 1993a). Andesites from Ruapehu have more radiogenic Sr isotope ratios than TVZ basalts, indicative of higher levels of crustal additions. Meta-sedimentary basement lithologies from within the TVZ exhibit a wide range in isotopic compositions, overlapping with the rhyolites and extending to considerably more radiogenic Sr isotope compositions (see Price et al., 2015). In general, the Waipapa Terrane has less radiogenic Sr isotope compositions than the older Torlesse sediments (Kaweka Terrane) and where there is an overlap, Waipapa lithologies tend to have more radiogenic Nd at a given Sr isotope ratio. Younger Torlesse sediments (Pahau Terrane) are more similar to the Waipapa Terrane. The metasedimentary basement samples

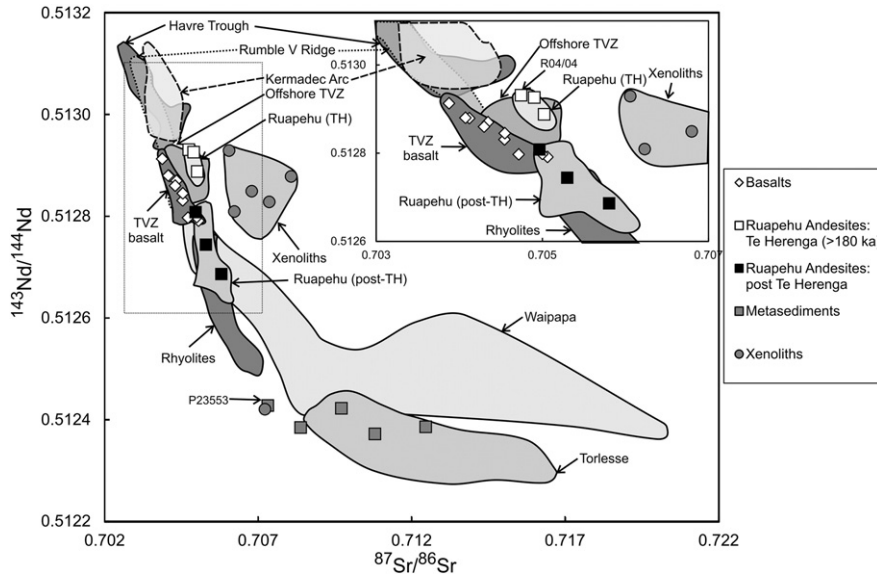


**Fig. 3.** Overview plot comparing Sr and Nd isotope data of the investigated samples with literature data from Kermadec Arc, Havre Trough and the TVZ (inset focuses on TVZ volcanics). TH = Te Herenga Formation (250–180 ka). Note that there is a general trend of increasing  $^{87}\text{Sr}/^{86}\text{Sr}$  and decreasing  $^{143}\text{Nd}/^{144}\text{Nd}$  from the Kermadec arc and Havre Trough, through the TVZ basalts and into the TVZ andesites and rhyolites. (Data sources: Adams and Maas (2004); Adams et al. (2008, 2009); Gamble et al. (1993a, 1994); Graham et al. (1992); McCulloch et al. (1994); Pearce et al. (2007); Price et al. (2005, 2012, 2015); Todd et al. (2010, 2011); Waight et al. (1999); Woodhead et al. (2001).)

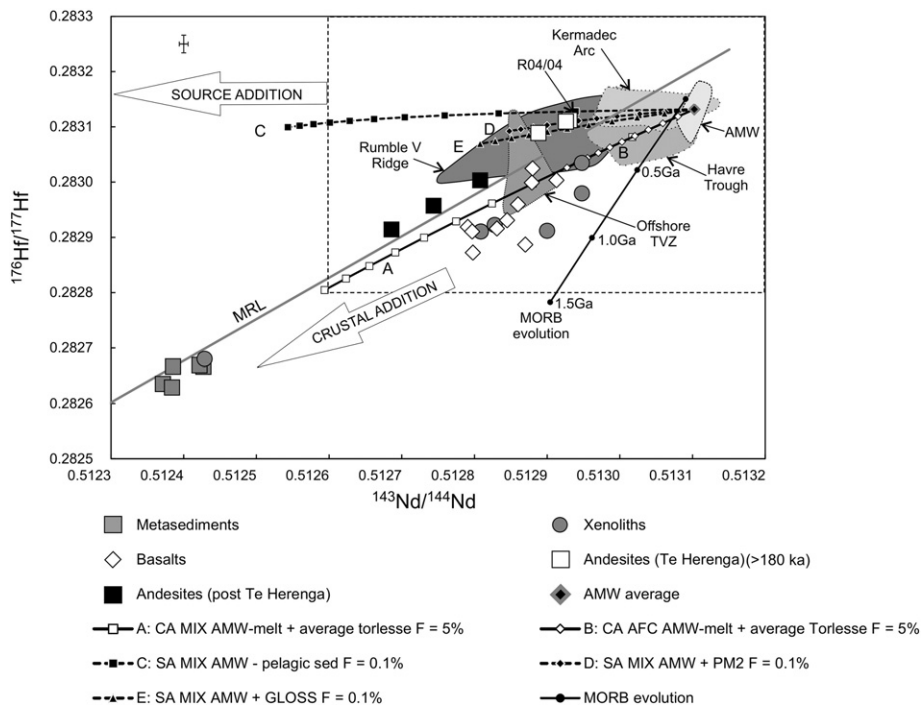


**Fig. 4.** Overview plot of  $^{176}\text{Hf}/^{177}\text{Hf}$  versus  $^{143}\text{Nd}/^{144}\text{Nd}$  for TVZ samples compared to volcanics from North of New Zealand (Kermadec, Rumble and Havre), with representative model curves illustrating the contrasting effects of crustal and source sediment additions. Crustal addition produces linear trends between end-members and sub-parallel to the mantle reference line, e.g. curve A = Bulk mixing between a melt derived from average ambient mantle wedge (AMW) and average Torlesse, while curve B = AFC trend between the same end members. Note that curves A and B overlap, reflecting the similar geochemistry of Hf and Nd. Curves C-E are bulk mixing trends representing sediment source addition to an average AMW. C = addition of pelagic sediment; D = addition of a subducted sedimentary melt and E = addition of global subducted sediment composition (GLOSS). Source addition generally produces data trends that cross the mantle reference line with a relatively constant Hf isotope composition. Isotopic and trace element compositions of end-member components used in modelling in this and subsequent figures, as well as data sources, are summarized in Table 2. All model curves in this and subsequent figures representing source addition (labelled SA) are presented using solid symbols and dashed lines, whereas models of crustal addition (labelled CA) use open symbols and solid lines. Increments of mixing in all source addition models are 0.1% to a maximum value of 1%, whereas on all crustal addition models tick marks represent increments of 5% mixing or F (amount of liquid remaining) for bulk mixing and AFC plots respectively, and is shown to a maximum of 50%. Data sources for Kermadec Arc, Havre Trough and offshore TVZ as in Fig. 3. MRL = mantle reference line of Vervoort et al. (1999). Isotopic evolution of ancient MORB was calculated using parameters described by Geldmacher et al. (2011). The model assumes derivation of the depleted MORB mantle source at 3.9 Ga from a CHUR source, then evolution of the source to 1.5, 1.0 and 0.5 Ga to yield a modern day average MORB composition ( $^{143}\text{Nd}/^{144}\text{Nd} = 0.51309$ ,  $^{176}\text{Hf}/^{177}\text{Hf} = 0.28315$ ) ( $\epsilon\text{Nd} = 8.83$ ,  $\epsilon\text{Hf} = 13.38$ ) using  $^{147}\text{Sm}/^{144}\text{Nd} = 0.21412$  and  $^{176}\text{Lu}/^{177}\text{Hf} = 0.038215$ . MORB melts derived from these sources evolve using average MORB parent-daughter ratios (i.e.  $^{147}\text{Sm}/^{144}\text{Nd} = 0.1986$  and  $^{176}\text{Lu}/^{177}\text{Hf} = 0.027$ ). Error bars represent estimated reproducibility based on replicate analyses of standards. The dashed square highlights the area examined in more detail in Fig. 6.

analysed have  $^{87}\text{Sr}/^{86}\text{Sr} = 0.70732\text{--}0.71246$  and  $^{143}\text{Nd}/^{144}\text{Nd} = 0.51243\text{--}0.51237$  ( $\epsilon\text{Nd} = -4.0$  to  $-5.0$ ) and agree well with literature data and with average Kaweka Terrane as proposed by Price et al. (2015). The single sample identified as representing the Waipapa Terrane (P23553) plots outside the previous compilations of both Torlesse and Waipapa data, with somewhat less radiogenic Sr than most Torlesse samples and less radiogenic Nd than most Waipapa samples. A metasedimentary xenolith included with Ruapehu andesites has Sr and Nd isotopic compositions similar to the metasedimentary basement samples. The Ruapehu meta-igneous granulite xenoliths have relatively radiogenic and distinctive Sr and Nd isotopic ratios ( $^{87}\text{Sr}/^{86}\text{Sr} = 0.70611\text{--}0.70797$ ,  $^{143}\text{Nd}/^{144}\text{Nd} = 0.51281\text{--}0.51295$ ,  $\epsilon\text{Nd} = +3.5$  to  $+6.2$ ) (Fig. 3) – their unusual isotopic compositions were attributed by Graham et al. (1990) to possible seawater contamination of oceanic crust.

New Hf isotope data for volcanics from the TVZ and associated basement lithologies are presented in Table 1 and Figs. 4 and 5. The volcanic samples show a range in Hf isotopes from  $^{176}\text{Hf}/^{177}\text{Hf} = 0.28311$  to  $0.28287$  (equivalent to  $\epsilon\text{Hf} = +11.6$  to  $+3.1$ ), which overlaps with and extends to less radiogenic compositions than the Kermadec Arc and Havre Trough. In detail, the basalt samples have  $^{176}\text{Hf}/^{177}\text{Hf} = 0.28287\text{--}0.28303$  and  $^{143}\text{Nd}/^{144}\text{Nd} = 0.51279\text{--}0.51291$  ( $\epsilon\text{Hf} = +3.5$  to  $+8.9$ ,  $\epsilon\text{Nd} = +3.0$  to  $+5.4$ ) and define a trend that is below and at an angle to the mantle reference line of Vervoort et al. (1999). Ruapehu samples have more radiogenic Hf at a given  $^{143}\text{Nd}/^{144}\text{Nd}$  than the TVZ basalts and display a trend from  $^{176}\text{Hf}/^{177}\text{Hf} = 0.28291\text{--}0.28311$  and  $^{143}\text{Nd}/^{144}\text{Nd} = 0.51269\text{--}0.51293$  ( $\epsilon\text{Hf} = +8.9$  to  $+11.6$ ,  $\epsilon\text{Nd} = +1.1$  to  $+11.6$ ). The Ruapehu basalt sample has Hf and Nd isotopic compositions distinct from other TVZ basalts (more radiogenic Hf) and overlaps with the older Te Herenga andesites (consistent with the recently determined age of Conway et al., 2016), whereas the younger post-Te Herenga andesites are offset to less radiogenic Hf and Nd. The meta-sedimentary basement samples plus a meta-sedimentary xenolith from Ruapehu are less radiogenic than the volcanics and show only limited variation ( $^{176}\text{Hf}/^{177}\text{Hf} = 0.28263\text{--}0.28268$  and  $^{143}\text{Nd}/^{144}\text{Nd} = 0.51237\text{--}0.51243$  ( $\epsilon\text{Hf} = -3.7$  to  $-5.5$ ,  $\epsilon\text{Nd} = -3.9$  to  $-5.0$ )). Granulitic xenoliths from Ruapehu plot below the mantle reference line with  $^{176}\text{Hf}/^{177}\text{Hf} = 0.28291\text{--}0.28303$  and  $^{143}\text{Nd}/^{144}\text{Nd} = 0.51281\text{--}0.51295$  ( $\epsilon\text{Hf} = +4.4$  to  $+8.8$ ,  $\epsilon\text{Nd} = +3.5$  to  $+6.2$ ) and have ratios similar to those of the TVZ basalts. In a plot of  $^{176}\text{Hf}/^{177}\text{Hf}$  versus  $^{87}\text{Sr}/^{86}\text{Sr}$  (Fig. 5) it is apparent that TVZ basalts, post-Te Herenga Ruapehu andesites and granulitic xenoliths have

overlapping Hf isotopes but show a wide range of Sr isotope ratios. The Te Herenga andesites are distinguished by both more radiogenic Sr and Hf than the TVZ basalts.

#### 4. Discussion

The highly coupled geochemical behaviour of Hf and Nd during most fractionation and contamination processes is clearly illustrated in Fig. 4 where curves A and B represent mixing and AFC between a potential asthenospheric mantle melt and average TVZ metasediment. Both models are close to linear ( $r^2$  of 0.999), but differ due to the increased influence of the crustal component in the bulk mixing model. Because the metasedimentary crustal components in the TVZ show relatively restricted Hf and Nd isotope ratios, we can extrapolate through continental volcanic compositions to provide constraints on the isotope variations of the primary magmas. Moreover, the geochemical similarity of Hf and Nd also results in most igneous and crustal rocks plotting on a linear array (e.g., the terrestrial array of Vervoort et al. (1999)) (Fig. 4). On a global scale, this array is in reality a linear data cloud, with variations reflecting decoupling of Nd and Hf isotope compositions following differential behaviour of Lu/Hf and Sm/Nd during for example mantle metasomatism (Scott et al., 2014; Stracke et al., 2011) or retention of HREE in garnet (e.g. Blachert-Toft et al., 2005). On a local and regional scale however, the terrestrial array provides an important reference line, as most isotopic variations due to interactions between mantle and crustal end-members will be sub-parallel to this array.

Of particular relevance to our study is the spread in Hf and Nd isotope compositions oblique to the mantle reference line in the oceanic Kermadec Arc. These are potentially primary magma compositions in the TVZ and their variation has been attributed addition of a slab-derived flux, including small amounts of pelagic sediment or sedimentary melt formed in the presence of residual accessory minerals (Todd et al., 2010, 2011). Residual zircon (Hf-rich with low Lu/Hf) and other accessory minerals result in significantly fractionated Lu/Hf in partial melts relative to the residue. Deep-sea pelagic sediments are clay-rich and zircon-poor and thus have high REE concentrations and higher Lu/Hf but similar Sm/Nd compared to typical continental crust. This results in relatively radiogenic Hf compositions that are offset to the left of the main terrestrial array, whereas terrigenous sediments derived from continental erosion have Hf-Nd isotope characteristics similar to those of continental crust (Patchett et al., 1984). The higher concentrations of Hf and Nd in marine sediments (e.g., average global subducting

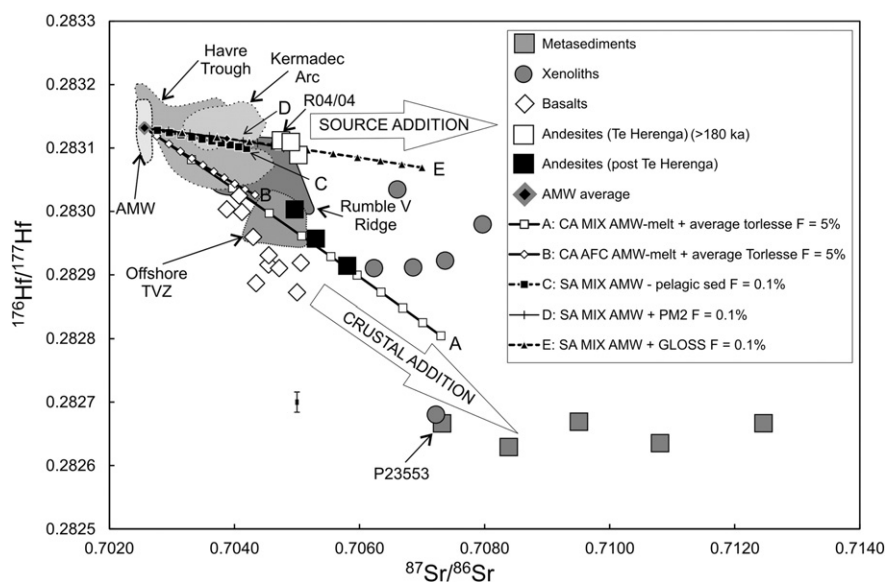


Fig. 5. Overview plot of  $^{176}\text{Hf}/^{177}\text{Hf}$  versus  $^{87}\text{Sr}/^{86}\text{Sr}$  for TVZ samples compared to volcanics from North of New Zealand (Kermadec, Rumble and Havre). Model curves illustrating the contrasting effects of crustal addition (curves A & B) and source addition of sediment (curves C-E) are shown. See caption of Fig. 4 and Table 2 for details of model end-members and data sources.

sediment = 4.1 ppm Hf and 27 ppm Nd; Plank and Langmuir, 1998) compared with typical mantle peridotite (depleted MORB mantle; DMM = 0.20 ppm Hf and 0.71 ppm Nd; Salters and Stracke, 2004) means addition of only small amounts (<1%) of sediment during source addition produces large changes in the isotopic compositions of the mantle source. Compositional variations that deviate from the mantle Nd-Hf isotopic array in some arcs have been attributed to variable source addition of pelagic sediment components (e.g., Handley et al., 2007; Yodzinski et al., 2010) and these effects can be further accentuated by the presence of residual minerals (e.g. zircon, monazite) during partial melting of subducting sediment (e.g., Martindale et al., 2013; Skora and Blundy, 2012). These minerals typically retain Hf, resulting in an increased Hf/Nd in the component added during source addition (e.g., Skora and Blundy, 2010; Turner et al., 2009). The general effects of sediment source addition are illustrated in models C-E in Fig. 4. These models demonstrate how the contrasts in isotopic composition and trace element concentrations between mantle peridotite and subducted sediment or melts mean that small amounts of sediment source addition cause large shifts in Hf-Nd isotope space across the mantle reference line. These shifts contrast with those resulting from crustal level processes where sediment involvement produces shifts parallel to the mantle reference line, and considerably smaller changes relative to the amount of sediment added (note the 50 fold increase in increments of mixing between source (e.g. trends C-E) and crustal addition models (e.g. trend A) in Fig. 4).

Todd et al. (2010, 2011) provide evidence for source addition in the Kermadec Arc and Havre Trough north of NZ and these studies provide a fundamental background for our interpretation of the TVZ isotope and trace element data. It is likely that similar variations in primary mantle-derived melts due to source addition occur beneath the TVZ. Two questions then arise: firstly, can these source variations be distinguished from the isotopic imprints of crustal assimilation? and secondly do these variations vary with geographic location, composition or relative volume of magmatism? In the following sections, we discuss the Sr, Hf and Nd isotope variations observed in our data set. We begin with the basement metasediments and lower crustal xenoliths to constrain potential crustal endmember compositions present during transit of the magmas through the lithosphere. We then discuss the observed variations in TVZ basalts and Ruapehu andesites in light of previous models, and assess the effects of source versus crustal addition during magma genesis.

#### 4.1. Basement lithologies

Basement in the TVZ is subdivided into two distinct meta-sedimentary terranes: the Permian to Cretaceous meta-greywackes and argillites of the eastern Torlesse Composite Terrane, comprising the Kaweka and Pahau Terranes; and the more primitive, arc-derived meta-sediments of the Jurassic Waipapa Terrane to the west (Fig. 2). The boundary between the two terranes lies west of Ruapehu (Mortimer et al., 1997) and, importantly, many previous studies on TVZ volcanics have demonstrated that Torlesse meta-sediments or their metamorphic equivalents are the most likely source for mid-upper crustal contamination during magmatism (Barker et al., 2014; Blattner and Reid, 1982; Charlier et al., 2010; Cole et al., 2000; Gamble et al., 1993a; McCulloch et al., 1994; Price et al., 2005, 2007, 2010, 2012). Several detailed studies have also shown that melting of mid-lower crustal plutonic equivalents to the volcanics contributed to the andesitic and rhyolitic magmas (e.g., Charlier et al., 2005, 2008, 2010; Price et al., 2005, 2012). Because these plutonics have isotopic and trace element compositions similar to those of the exposed volcanics, their involvement as a source and/or contaminating component is difficult to identify using conventional whole rock geochemistry.

Meta-sedimentary basement samples display a limited variation in  $^{143}\text{Nd}/^{144}\text{Nd}$  and agree well with previous data from the Kaweka

Terrane portion of the Torlesse Composite Terrane (e.g., Price et al. (2015) and references therein). The sample identified as representing the Waipapa Terrane (P23553) has a composition similar to the Torlesse and less radiogenic Nd than most Waipapa samples. It also has trace element characteristics that are more typical of Torlesse Composite Terrane sediments rather than Waipapa Terrane (i.e. La/Sc and Ti/Zr, see Fig. 4a in Mortimer et al., 1997). The sample was collected near the proposed Waipapa-Torlesse boundary and its exact affiliation is therefore unclear. A meta-sedimentary xenolith from Ruapehu (R97/104X) has Sr, Nd and Hf isotopic compositions similar to other meta-sediments, consistent with an origin from lithologies similar to those exposed at the surface. In summary, the data for the meta-sedimentary basement samples indicate that the mid-upper crustal meta-sediment component contributing to magmas during crustal addition is restricted in terms of Hf-Nd isotope compositions.

Another potential crustal component to affect TVZ magmatism are high-grade metamorphic rocks that occur as xenoliths in Ruapehu and Tongariro andesites (Graham et al., 1988, 1990; Price et al., 2005, 2010, 2012). Metamorphic equivalents of the meta-sedimentary basement (e.g. sample R97/104X) and residues from their partial melting dominate, and meta-igneous granulitic xenoliths, interpreted to represent lower crust underlying the meta-sediments, make up ca. 15% of the metamorphic xenolith population at these sites (Graham et al., 1990). Their Sr and Nd isotopic signatures, coupled with relatively heavy O isotope compositions led Graham et al. (1990) to conclude that the meta-igneous xenoliths represent hydrothermally altered oceanic crust with addition of small amounts of a sedimentary component that originated as underthrust material or as remnants of the original oceanic crust onto which the original Torlesse sediments were deposited. The unique composition of these xenoliths is apparent in plots of Sr versus Nd and Hf isotopes (Figs. 4 & 5) where they are clearly distinct from both volcanic and metasedimentary samples and they have been invoked to explain particular aspects of geochemical variation in the Ruapehu andesites (Price et al., 2012), a topic we will return to below. Hf isotope compositions of the xenoliths are consistent with an origin as oceanic basaltic crust as proposed by Graham et al. (1990). In Fig. 4, a trend representing predicted present day compositions of MORB generated at various times in the past (0.5, 1.0 and 1.5 Ga) is plotted (see figure caption for details) and although it does not coincide with the Ruapehu meta-igneous xenoliths, it defines a broadly parallel trend. Two options can be suggested to explain this: Addition of small (<5%) amounts of sediment to ancient MORB will drag compositions to the left (i.e. to lower  $\epsilon\text{Nd}$  and potential overlap with the Ruapehu xenoliths), which is also consistent with the suggestion that a sedimentary component is needed to explain the Sr, Nd and O isotope systematics of the granulite xenoliths (Graham et al., 1990). It is also feasible that the source for the MORB component was not typical depleted mantle as modelled in Fig. 4, but was instead more enriched and E-MORB-like (e.g. ca.  $^{177}\text{Hf}/^{176}\text{Hf} = 0.28308$  ( $\epsilon\text{Hf} = +11$ ),  $^{143}\text{Nd}/^{144}\text{Nd} = 0.51285$  ( $\epsilon\text{Nd} = +6$ )) (Hofmann, 2003). Isolated Carboniferous basalt slivers within the oldest Torlesse may represent preserved fragments of the oceanic crust on which it was deposited (Mortimer, 2004) and thus represent less-metamorphosed equivalents of the Ruapehu xenoliths. These rocks, now metamorphosed to prehnite-pumpellyite to greenschist facies assemblages, have modern-day  $\epsilon\text{Nd}$  dominantly between +5 and +6 (Bierlein and Craw, 2009) broadly overlapping the Ruapehu xenoliths. Furthermore, the Carboniferous basalts often have immobile trace element compositions indicative of E-MORB, and a ‘within plate’ signature (i.e. somewhat LREE-enriched patterns), which is consistent with a more enriched origin than the MORB trend modelled in Fig. 4 (Bierlein and Craw, 2009). Assuming a typical depleted source with small amounts of sediment contamination for the meta-igneous xenoliths, the trend in Fig. 4 would suggest an approximate age of this MORB between 0.5 and 1 Ga. This, in turn, would be broadly consistent with the Permian to Cretaceous age of the overlying sediments, although we note that if this MORB

component was derived from a more enriched source then its age would likely be younger.

Our data thus show that the dominant metasedimentary crust in the TVZ has relatively homogenous Nd and Hf isotopic compositions; therefore it should be possible to extrapolate from these metasedimentary compositions, through volcanic data arrays, towards more primitive compositions to identify potential variations in the composition of primary magmas entering the lithosphere. In the case of Ruapehu eruptives, the meta-igneous xenoliths represent a component with a unique Sr, Nd and Hf isotope composition that should also be readily identifiable as a potential crustal contaminant. Having characterised potential crustal components in the TVZ, we can now turn our attention to composition variations in the volcanic rock samples and we discuss the data for basalts and andesites below.

#### 4.2. Basalts

Isotopic compositions of TVZ basalts spread from overlapping with the southernmost Kermadec arc volcanics towards more radiogenic  $^{87}\text{Sr}/^{86}\text{Sr}$  and lower  $^{143}\text{Nd}/^{144}\text{Nd}$  (Fig. 3). These variations have been interpreted to reflect AFC-style interactions between Kermadec arc-like magmas with Torlesse meta-sedimentary crust beneath the TVZ (Gamble et al., 1990, 1993a). Similarly, Gamble et al. (1994), Macpherson et al. (1998) and Todd et al. (2011) have shown that basalts at the oceanic-continent transition off-shore of the TVZ have Sr, Nd, Hf and O characteristics indicative of crustal contamination. Based on detailed modelling of source addition processes under the TVZ, Rooney and Deering (2013) put forward the alternative argument that northwards increasing LILE abundances in the TVZ basalts reflect melting of a MORB-type mantle source modified by progressive addition of slab-derived components from subducted sediments and altered oceanic crust; crustal contamination was not considered in their modelling. TVZ basalts have Hf-Nd isotopic compositions that form an array that scatters below and oblique to the mantle reference line (Fig. 4). Their compositions are distinctly less radiogenic than basalts from the Kermadec Arc and Havre Trough, and overlap with and extend to less radiogenic compositions than basalts from the offshore TVZ and are broadly consistent with crustal contamination processes (Figs. 3 and 4). The Ruapehu basalt (R04/04) is distinct from the other central TVZ basalts in Hf-Nd-Sr isotope space and more similar to the older Ruapehu andesites (Te Herenga Formation) and will be discussed in conjunction with those below.

TVZ basalts have Hf and Nd isotopic compositions that overlap with the lower crustal granulitic xenoliths from Ruapehu (Fig. 4). Involvement of these as a crustal contaminant or source component in the basalts is deemed unlikely as a) it would require large degrees of contamination (approaching 100%) which should also be evident in major and trace element chemistry of the basalts, and b) the xenoliths have unusually radiogenic Sr isotope compositions, but no appreciable shift to radiogenic Sr is observed in the TVZ basalts. Moreover, the xenoliths have relatively heavy oxygen isotope compositions ( $\delta^{18}\text{O} = +8$  to  $+12$ , Graham et al., 1990) and thus large amounts of granulitic component would shift the basalts to higher  $\delta^{18}\text{O}$  than observed ( $+5.8$  to  $+6.7$  - Blattner and Reid, 1982). Lastly, the granulite xenoliths are only found in the Ruapehu-Tongariro region and their extent and significance to the north are not well defined, which leads us to focus on the role of metasedimentary components in causing chemical variations in the TVZ basalts.

Selected mixing and AFC models for various end member compositions are presented in Fig. 6 (see Table 2 for details). Representative source addition models show mixing between ambient mantle wedge compositions defined by Todd et al. (2011) and partial melts of subducted sediments (Fig. 6A, curves A and B) or bulk mixing with Torlesse sediment (Fig. 6A, curves C and D). The two sediment partial melt compositions are chosen to represent the extremes of values considered by Todd et al. (2010). Source addition of bulk Torlesse is modelled as this is likely to dominate the eroded sediment flux into

the trench east of the North Island (Carter et al., 1996). Similar trends are generated when using an average global subducted sediment composition, e.g.  $\varepsilon\text{Hf} = +2$ ,  $\varepsilon\text{Nd} = -9$  (Chauvel et al., 2008). Note that these trends represent 0.1% increments of addition of the crustal component. It is clear that source addition of small amounts of sediment to the mantle can produce significant variations in isotope composition. Representative crustal addition models are represented by AFC trends involving partial melts derived from various ambient mantle wedge compositions (assuming MORB-like trace element compositions) assimilating average Torlesse type compositions (Fig. 6B, curves E and F). The full spread in Nd and Hf isotope values amongst the TVZ basalts is impossible to recreate with any single model of source addition (models A-D) or crustal addition (models E & F) involving any unique pair of discrete mantle and crustal end-members. Similarly, variations in Sr-Hf isotope space cannot be explained by source or crustal addition models using ambient mantle wedge compositions and subducted Torlesse sediments, or melts thereof (Fig. 5). In particular, all modelled trends with Torlesse as the added crustal component are sub-parallel to the mantle reference line (e.g. Fig. 6A & B, curves C-F) whereas those involving partial melts of sediment have relatively constant  $^{176}\text{Hf}/^{177}\text{Hf}$  with changing  $^{143}\text{Nd}/^{144}\text{Nd}$ . None of the models, however, recreate the steeply positively inclined trend defined by the TVZ basalt data. Source addition of small amounts (<1%) of partial melt of subducted sediment to the ambient mantle wedge (Fig. 6A, curves A and B) as proposed by Todd et al. (2010, 2011) for the Kermadec Arc, cannot explain even the most isotopically enriched TVZ basalt compositions. However, addition of bulk sediment with a composition of average Torlesse to end-member ambient mantle wedge compositions (e.g., Fig. 5 curves A-B, Fig. 6A curves C-D) can better explain the TVZ basalts with the most mantle-like Sr, Nd and Hf isotope signatures, although relatively large amounts of sediment added to the mantle source would be required (e.g. >1%). Source addition of Torlesse can, in turn, not explain TVZ basalts with less radiogenic Nd and Hf and more radiogenic Sr. The relatively heavy oxygen isotope compositions in both the onshore TVZ basalts ( $\delta^{18}\text{O}$  of 5.8 to 6.7 in Blattner and Reid, 1982) and offshore TVZ (Macpherson et al., 1998) are also inconsistent with source contamination and crustal level contamination processes are apparently required.

Crustal addition of metasediment to pristine melts of ambient mantle wedge compositions also cannot explain the isotopic variations in TVZ basalts in full. AFC models involving melts derived from various ambient mantle wedge compositions without source addition and bulk Torlesse sediment (Fig. 5 curves A-B, Fig. 6B, curves E and F) approach TVZ basalt compositions but require high degrees of fractionation (50% or higher) or bulk mixing (20%, see also Fig. 4), which is inconsistent with the low  $\text{SiO}_2$  contents and close to primitive nature of many of the basalts (Gamble et al., 1993a). Furthermore, such purely crustal models fail to reproduce the Sr-Hf isotope array (Fig. 5) and trend to lower  $^{87}\text{Sr}/^{86}\text{Sr}$  at a given  $^{176}\text{Hf}/^{177}\text{Hf}$ .

The TVZ basalts appear to require input of sedimentary material both at source as well as in the lithosphere. However, even then it remains difficult to explain the whole range of Hf-Nd isotope variation via addition of Torlesse to a single source-contaminated primary magma. The array of Hf and Nd isotopic compositions in the TVZ basalts could be explained by crustal contamination of a mantle-derived component with ca.  $^{176}\text{Hf}/^{177}\text{Hf} = \text{ca. } 0.2831$  and  $^{143}\text{Nd}/^{144}\text{Nd} = \text{ca. } 0.5139$ . Potential mantle-derived end-members are present in the Kermadec Arc and Rumble Ridge and these have Hf-Nd compositions consistent with source addition of subducted sediment melt (Todd et al., 2011). However, a compositionally appropriate crustal end-member would plot significantly below the mantle reference line with relatively unradiogenic Hf at a given  $^{143}\text{Nd}/^{144}\text{Nd}$ . Such compositions are distinct from the Torlesse and, other than the granulite xenoliths (excluded above), are unknown in the TVZ. Model contamination curves between Kermadec-like and Torlesse end-members would need to be strongly curved (concave up) to mimic the data array defined

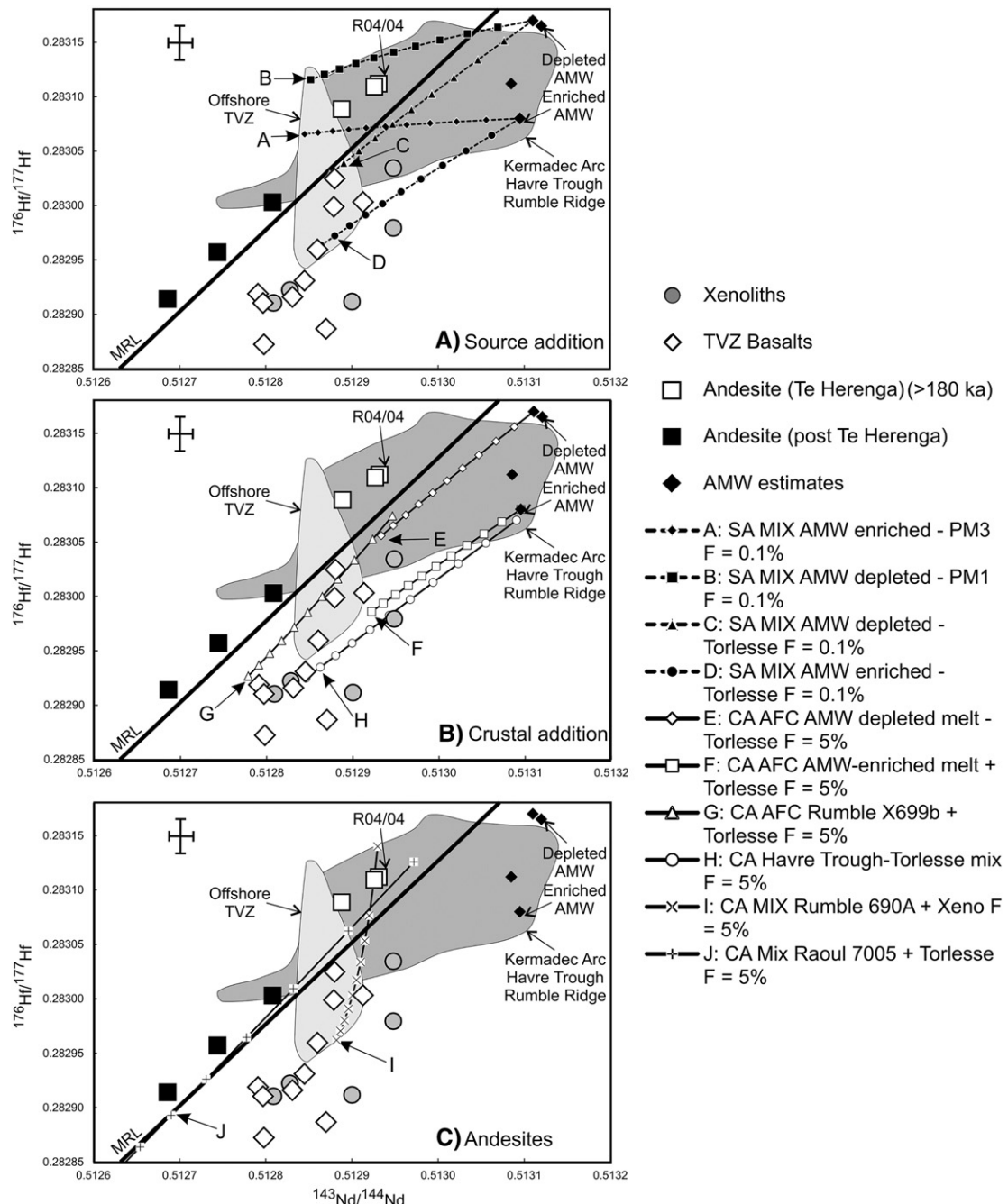


**Fig. 6.** Plot of  $^{176}\text{Hf}/^{177}\text{Hf}$  vs  $^{143}\text{Nd}/^{144}\text{Nd}$  focusing on TVZ volcanics; details of model end-members and data sources are given in the caption of Fig. 4 and Table 2. Curves A–H represent possible models to explain variations in the TVZ basalts and illustrate that both source and crustal addition is required. A) Source addition models for basalts. Curves A and B represent source addition bulk mixing models between selected partial melts of subducted sediment (PM1 and PM3) with enriched and depleted end-member AMW compositions. Curves C and D represent source addition bulk mixing models using average bulk Torlesse (see Fig. 4) with AMW. B) Crustal addition models for basalts. Curves E and F represent AFC models of crustal addition of bulk Torlesse to melts derived from AMW. Curves G and H are selected AFC models simulating crustal addition of bulk Torlesse to parental magmas where the source has undergone source addition of sediment. Magmatic end-member in curve G is sample X699B from Rumble V Ridge (Todd et al., 2010), and in curve H it is sample 987-9 from the Havre Trough. C) Models to explain isotope variations in Ruapehu andesites. Curve I represents mixing between a representative source contaminated Kermadec Arc-Rumble Ridge composition (X690A) with an average meta-igneous xenolith composition. Curve J represents mixing between Raoul sample 7005 (from Pearce et al., 2007) and bulk Torlesse.

by TVZ basalts and require a radical and unusual change in chemistry, i.e. changing  $K$  values from typical values close to 1 to 0.3–0.4. This can theoretically be accomplished by invoking an unrealistic three-fold increase in Hf concentrations in the crustal contaminant, e.g. by changing Hf/Nd from 5.7 ppm/28.8 ppm to 15 ppm/28.8 ppm, or alternatively, by changing the Hf/Nd in the magmatic component from 2.0 ppm/9.8 ppm to 0.6 ppm/9.8 ppm.

Crustal addition models in Figs. 4–6 assume bulk addition of metasedimentary crust, however several authors have noted that

disequilibrium partial melting and retention of residual minerals can result in contaminants with isotopic and trace element characteristics distinct from bulk rock compositions (e.g., Ayres and Harris, 1997; Davies and Tommasini, 2000; Knesel and Davidson, 1996; Meade et al., 2014; Waight and Lesher, 2010). Such processes could potentially change the Hf/Nd in the contaminating end-member. The main host of Hf in meta-sedimentary lithologies is zircon; however retention of residual zircon during partial melting is not a viable mechanism to produce contamination curves that mimic the trends defined by TVZ basalts. Zircon

**Table 2**

End-member compositions and parameters used in AFC and mixing models.

	$^{87}\text{Sr}/^{86}\text{Sr}$	Sr (ppm)	$^{143}\text{Nd}/^{144}\text{Nd}$	Nd (ppm)	$^{176}\text{Hf}/^{177}\text{Hf}$	Hf (ppm)
Ambient Mantle Wedge (AMW) <sup>a</sup>	0.70256	7.664	0.51310	0.581	0.28313	0.157
AMW enriched <sup>a</sup>	0.70260	7.664	0.51310	0.581	0.28308	0.157
AMW depleted <sup>a</sup>	0.70255	7.664	0.51311	0.581	0.28317	0.157
AMW melt <sup>b</sup>	0.70256	140.0	0.51310	10.90	0.28313	2.64
AMW melt enriched <sup>b</sup>	0.70260	140.0	0.51310	10.90	0.28308	2.64
AMW melt depleted <sup>b</sup>	0.70255	140.0	0.51311	10.90	0.28317	2.64
X699B (Rumble) <sup>c</sup>	0.70387	276.0	0.51295	8.19	0.28307	1.38
X690A (Rumble) <sup>d</sup>	0.70342	323.0	0.51293	7.35	0.28314	0.96
Raoul 7005 <sup>e</sup>	0.70349	186.5	0.51305	6.90	0.28310	1.30
Havre Trough 987-9 <sup>c</sup>	0.70315	168.0	0.51309	6.60	0.28307	1.39
Pelagic sediment <sup>c</sup>	0.70952	233.0	0.51234	158.20	0.28296	3.51
Pelagic sediment melt 1 <sup>d</sup>	0.70954	445.2	0.51248	39.83	0.28277	2.47
Pelagic sediment melt 2 <sup>d</sup>	0.70954	445.2	0.51248	39.77	0.28277	1.94
Pelagic sediment melt 3 <sup>d</sup>	0.70954	445.3	0.51248	39.34	0.28277	0.77
GLOSS <sup>f</sup>	0.71730	327.0	0.51218	27.00	0.28283	4.06
Torlesse <sup>g</sup>	0.70929	334.0	0.51240	28.60	0.28266	5.98
Average granulite xenolith <sup>h</sup>	0.70693	378.0	0.51284	8.30	0.28291	3.30
Bulk D used for AFC models <sup>i</sup>		0.4487		0.0303		0.0495

a) From Todd et al. (2011), with trace element concentrations of average MORB mantle from Workman and Hart (2005).

b) From Todd et al. (2011), with trace element concentrations of global MORB from Arevalo and McDonough (2010).

c) From Todd et al. (2011).

d) From Todd et al. (2010).

e) From Smith et al. (2010) and Pearce et al. (2007).

f) Global subducting sediment from Chauvel et al. (2008) and Plank and Langmuir (1998).

g) Average of five metasediments + xenolith R97/104X (this study).

h) Isotopic compositions (this study) trace elements from Price et al. (2012).

i) Assuming a crystallising assemblage of 59% olivine, 24% plagioclase, 9% orthopyroxene, 7% clinopyroxene and 1% (average of models 1, 2 and 4 in Gamble et al., 1990), partition coefficients compiled in Claeson and Meurer (2004) and an r value of 0.2.

retention during partial melting will decrease Hf/Nd in contaminant melts and produce mixing and AFC curves similar to those used as evidence for source addition in the Kermadec Arc (Todd et al., 2010, 2011). Moreover, the relatively low Lu/Hf of zircon yields unradiogenic Hf over time compared to bulk rock compositions, thus derivative melts will be likely to have more radiogenic Hf (Chen et al., 2015). Thus crustal addition of partial crustal melts involving residual zircon will tend to mimic source addition involving partial melts of sediments, pulling compositions towards higher  $^{176}\text{Hf}/^{177}\text{Hf}$  at any given  $^{143}\text{Nd}/^{144}\text{Nd}$ . Therefore, disequilibrium crustal melting involving residual zircon also fails to explain the spread in TVZ basalt compositions towards lower εHf and εNd. We note that Sr, Nd and Pb isotope models for crustal contamination of TVZ volcanics generally fit well if bulk rock compositions are used as contaminants (e.g., Gamble et al., 1993a; Graham et al., 1995; McCulloch et al., 1994; Price et al., 2012) and there is thus limited evidence to entertain disequilibrium crustal melting further in our discussion. Finally, inherited zircon populations in TVZ dacites and rhyolites are also consistent with derivation from bulk assimilation of Torlesse greywackes and indicate that crustal melting reaches degrees where zircon is released and incorporated into the magmatic systems (e.g., Barker et al., 2014; Brown and Smith, 2004; Charlier et al., 2010; McCormack et al., 2009).

It is clear that the Hf-Nd isotope compositions of TVZ basalts are difficult to explain through interactions between a single mantle-derived end-member (with or without source addition) and Torlesse metasediments. The tendency for crustal addition to produce straight line contamination trends parallel to the mantle reference line contrasts markedly with the oblique Hf-Nd isotope trend displayed by the TVZ basalt data. Extrapolating such contamination trends through individual basalt compositions towards more radiogenic and uncontaminated compositions indicates that there may have been an array of parental magma compositions prior to crustal interactions and Hf-Nd isotope heterogeneity of TVZ basalts points to parental magmas with up to 1% of source addition (either sediment melt or bulk Torlesse). This creates an array of parental magma compositions to the right of ambient mantle wedge compositions (Figs. 4 and 6A) which notably mimic the parental magma compositions seen in the Kermadec Arc. This model then clearly implies that no single primary melt composition can be assumed for all

of the TVZ basalts. Rather, there must be variable inputs from subducted sediments to the mantle sources and potentially also variations in the ambient mantle wedge itself. Mantle-derived magmas from these variable sources have then experienced further interactions with Torlesse-like crustal components at lithospheric levels, producing contamination trends sub-parallel to the mantle reference line. These processes are illustrated qualitatively in Fig. 4. Two examples of AFC between Torlesse and potential mantle melts are presented in Fig. 6B. Curve G uses basalt from the Rumble Ridge with Hf and Nd isotopic compositions consistent with source contamination by either 0.5% of a sedimentary partial melt or 0.6% bulk Torlesse as the parental magma. Relatively small amounts of AFC (10–15% crystallisation) involving a Torlesse crustal contaminant can explain the most radiogenic TVZ basalts. Curve H in Fig. 6 represents AFC between Torlesse and a Havre Trough sample that has Hf and Nd compositions close to enriched ambient mantle wedge with little influence from subducted sediments, and approximates the less radiogenic Hf and Nd compositions of the TVZ basalts. This model requires relatively high degrees of crystallisation, and this could be reduced by increasing the amount of sediment added during crystallisation (high 'r') and/or through source addition of small amounts of bulk Torlesse (e.g. curve D, Fig. 4). These models replicate most of the spectrum of TVZ basalt compositions and require lower degrees of crystallisation (20–40%) than is the case for contamination of unmodified ambient mantle-derived melts.

Rooney and Deering (2013) proposed variable addition of sediments to the mantle source to explain variable LILE contents in the TVZ basalts but did not consider crustal additions in their modelling as originally proposed by Gamble et al. (1993a). If the Rooney and Deering (2013) model is correct, we would expect to see a variation in Hf and Nd isotope compositions that cuts across the mantle reference line with similar  $^{176}\text{Hf}/^{177}\text{Hf}$  but decreasing  $^{143}\text{Nd}/^{144}\text{Nd}$  with increasing sediment input. The LILE-enriched nature of the Torlesse and continental crust in general (Price et al., 2015; Rudnick and Gao, 2003) means that crustal addition will have important implications for trace element compositions in contaminated magmas. Variations in isotopic composition and representative LILE-HFSE ratios (Rb/Zr, Ba/La) with location and SiO<sub>2</sub> are presented in Fig. 7. The data show broad trends towards less radiogenic Hf and Nd isotope ratios and increasing  $^{87}\text{Sr}/^{86}\text{Sr}$ , Rb/Zr and Ba/La

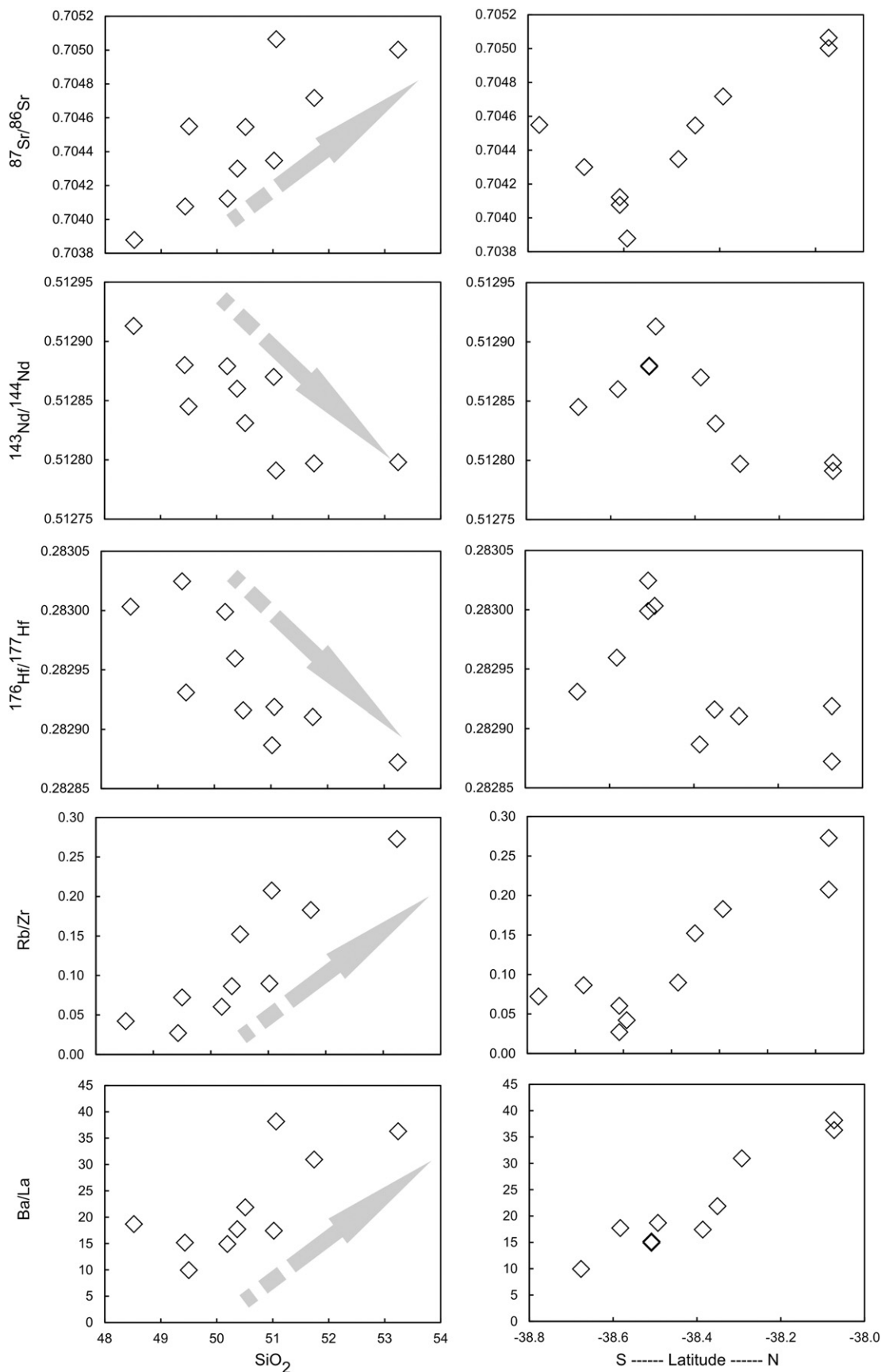


**Fig. 7.** Variation plots demonstrating correlations between isotopic compositions and representative LILE-HFSE ratios with location and silica content in Taupo Volcanic Zone basalts. Grey arrow shows trends expected as a consequence of AFC. The correlation indicates crustal differentiation and particularly crustal assimilation processes must have occurred during petrogenesis.

from south to north. While such trends are compatible with increasing addition of slab components to the mantle source, as proposed by Rooney and Deering (2013), these trends are also closely coupled to increasing SiO<sub>2</sub>, which clearly implies that the observed variations are in part linked to AFC-style differentiation processes at crustal levels. The trends suggest that northern TVZ basalts have the most unradiogenic Hf and Nd compositions and plot furthest from potential Kermadec arc parental compositions, whereas basalts from the south (e.g., Kakuki and Tatua) plot closer to the mantle reference line. This trend is the opposite to that proposed by Rooney and Deering (2013) as it suggests that the southernmost basalts have a larger source addition component, yet lesser degrees of crustal addition, compared to those in the north. The Hf-Nd isotope results presented here clearly complicate the conclusions of Rooney and Deering (2013), and illustrate the dangers of only using trace elements to characterise mantle sources for basalts and ignoring crustal level processes.

#### 4.3. Ruapehu andesites

Ruapehu volcano is one of the best characterised volcanoes in New Zealand (e.g., Conway et al., 2015, 2016; Gamble et al., 1999; Graham and Hackett, 1987; Nakagawa et al., 2002; Price et al., 2012) and was chosen to represent andesitic volcanism in the TVZ. Two major cone forming events are identified: (1) The older Te Herenga Formation (250–180 ka) has relatively restricted compositions with low K contents, and relatively unradiogenic Sr (<sup>87</sup>Sr/<sup>86</sup>Sr = 0.7048–0.7052) and radiogenic Nd (<sup>143</sup>Nd/<sup>144</sup>Nd = 0.51276–0.51292) isotope compositions (see Fig. 3). (2) The younger post-Te Herenga Formations have more variable compositions and display a shift to more radiogenic Sr and less radiogenic Nd isotopic compositions (<sup>87</sup>Sr/<sup>86</sup>Sr = 0.7047–0.7061, <sup>143</sup>Nd/<sup>144</sup>Nd = 0.51264–0.51293). The Ruapehu basalt has an isotopic composition that is similar to the Te Herenga andesites and is distinct from other basalts from the TVZ (Price et al., 2012) and in general the Te Herenga Formation has more radiogenic Sr at the same Nd isotopic composition as primitive TVZ basalts. Price et al. (2012) propose that this reflects interactions between primary mantle-derived magmas and lower crustal granulite, followed by limited interactions with Torlesse-type materials in the mid-crust. The younger Ruapehu lavas are argued to have had more prolonged residence times in the mid-to upper-crust and hence more opportunity for interaction with Torlesse-like meta-sediments (Price et al., 2012). In detail however, individual magma batches at Ruapehu are likely to have had complex histories involving storage in multiple magma chambers and various magma mixing and crustal contamination events (Gamble et al., 1999; Price et al., 2005, 2012). Random geochemical variations in Ruapehu eruptives over short time scales (e.g., Gamble et al., 1999), together with complex zoning in phenocrysts and heterogeneity in Sr isotope compositions in plagioclase (Price et al., 2012) are indicative of a complex crystal cargo of phenocrysts, antecrysts and xenocrysts reflecting variable residence times and different histories in multi-level dynamic magma chamber systems. These complexities are becoming increasingly recognised as typical for intermediate to evolved subduction zone magmas worldwide (e.g., Chadwick et al., 2007, 2013; Dahren et al., 2012; Davidson et al., 2005, 2007; Troll et al., 2013). Nevertheless, the evolution of andesites at Ruapehu, and particularly the post-Te Herenga andesites, can be broadly replicated by bulk mixing or AFC processes that involve local crust (e.g., Graham et al., 1995; Price et al., 2012; Waight et al., 1999).

Ruapehu samples form a linear array in Hf-Nd isotope space that is parallel to and just above the mantle reference line (Figs. 4, 6). As a first order observation, this indicates that the parental source for Ruapehu magmas cannot be derived directly from unmodified ambient mantle wedge and some source addition of sediment must be involved. The relatively radiogenic compositions of the Te Herenga samples also indicate that this source sediment component would more likely be partial sediment melt rather than bulk Torlesse sediments (see curves A-C

in Fig. 4). Variations in Sr-Hf-Nd isotopes also indicate that the TVZ basalts do not represent appropriate parental magma compositions for Ruapehu andesites as the former have distinctly less radiogenic Hf at corresponding values of <sup>87</sup>Sr/<sup>86</sup>Sr and <sup>143</sup>Nd/<sup>144</sup>Nd.

Geochemical modelling and petrographic observations indicate the Te Herenga magmas formed following interactions between depleted primary, mantle-derived magmas similar to those characterising the Kermadec Arc (especially Raoul volcano) and lower crustal meta-igneous granulitic compositions in a deep crustal hot zone (Price et al., 2005, 2012). However, in terms of Hf and Nd isotopes, magmas parental to the Te Herenga magmas have likely been derived from an ambient mantle wedge that was significantly modified by source sediment additions. No Kermadec data in the literature (including Raoul volcano) have Hf isotope compositions suitable to act as parental magmas for the Te Herenga magmas if it is assumed that a lower crustal granulite component is the only contaminant (Fig. 6). In Fig. 6C (curve I) we show that mixing between an Eastern Rumble sample (X690A from Todd et al. (2010) with Hf isotope compositions indicative of source contamination by ca. 0.5% sediment melt) and an average bulk xenolith composition can explain the Hf-Nd isotope composition of the Te Herenga magmas, with only ca. 5% mixing required. Although only three samples of the Te Herenga magmas have been analysed, the shift to less radiogenic Hf and Nd observed in the more evolved sample is easily explained by AFC-type processes with Torlesse in the mid-upper crust as suggested by Price et al. (2012). We plot mixing trends instead of AFC trends in Fig. 6C because Price et al. (2012) demonstrated that combinations of AFC and mixing are required to explain most Ruapehu compositions and the pure AFC trends require unrealistically high amounts of crystallisation. The Rumble sample chosen here as a primitive end-member for modelling has Sr and Nd isotopic compositions similar those used by Price et al. (2012) to model the evolution of the Te Herenga magmas. Consequently, the models we have developed here corroborate these previously published interpretations.

The Hf-Nd-Sr isotopic compositions of the Te Herenga Formation can also be explained with derivation of the whole suite from a parental melt derived from ambient mantle wedge source plus small amounts of subducted sediment melt (e.g. Figs. 5, 6A); there is no need to invoke lower crustal granulites as a crustal component as suggested by Price et al. (2012) on the basis of radiogenic isotopes. However, trace element compositions are more easily reconciled with addition of a lower crustal component and the common occurrence within the Te Herenga eruptives of meta-sedimentary and meta-igneous xenoliths from both lower and upper crust make a compelling case in favour of crustal additions.

The younger, post-Te Herenga (<160 ka) eruptives on Ruapehu are characterised by more radiogenic Sr isotope compositions than those observed in the Te Herenga Formation (see Fig. 3). In Hf-Nd isotope space, three analysed samples of post-Te Herenga andesite exhibit a striking linear array between the Te Herenga Formation towards Torlesse-type crustal compositions that parallels the mantle reference line (Fig. 6). This is broadly consistent with increased interaction with Torlesse meta-sediments in the mid-upper crust during the younger episodes of Ruapehu's volcanic development, as previously proposed by Price et al. (2012). Nevertheless, as already noted by Price et al. (2012), AFC trends using Ruapehu basalt as a starting composition are unable to replicate the Sr-Nd isotopic compositions of the post-Te Herenga andesites. Instead Price et al. (2012) show that AFC involving a primitive intra-oceanic arc basalt and either Torlesse or meta-igneous granulitic lower crust can better explain the more primitive post-Te Herenga andesites. This aspect is further underlined by the presence of granulitic xenoliths and mixed phenocryst populations (Price et al., 2012). In Fig. 6C (curve J) we demonstrate that contamination of a Kermadec magma with a relatively large amount of source sediment addition (e.g., sample 7005 from Raoul Island; Pearce et al., 2007) by Torlesse sediments can explain the Hf-Nd isotope compositions of the limited number of post-Te Herenga samples analysed

here. Involvement of lower crustal granulites will tend to move these mixing trends to the right on the Hf-Nd isotope plot as shown for the Te Herenga magmas, and therefore, a parental magma intermediate between that used to model the Te Herenga magmas and Raoul sample 7005 would also be appropriate. While we only provide an overview data set on this occasion, we conclude that the Hf-Nd isotope data are broadly consistent with previous models for the petrogenesis of Ruapehu volcanics presented by Price et al. (2012) with the additional, but significant qualification that there may be a need to consider source heterogeneity involving variable additions of a sediment component into the mantle wedge before generation of the primary magmas feeding into the Ruapehu magmatic system.

## 5. Conclusions and implications

- Variable degrees of source addition of sedimentary melts or bulk sediment to ambient mantle sources and shallow level crustal contamination are required to explain the variations in Hf and Nd isotopes observed in TVZ basalts and andesites. No single parental magma can be invoked to explain the isotopic variations in the investigated TVZ basalts, and each thus represents melting of a unique source.
- The TVZ basalts do not represent appropriate single-stage mafic end-members for more evolved magma compositions in the TVZ.
- Geographic variations in LILE/HFSE ratios in the basalts previously attributed to varying contributions from subduction-derived fluids (Rooney and Deering, 2013) also correlate with SiO<sub>2</sub> contents and isotopic compositions. This indicates that these variations dominantly reflect crustal contamination processes rather than variable source contributions.
- Variations in Hf and Nd isotopes in Ruapehu andesites are consistent with previously published models involving changing levels of crustal contamination. An early lower crustal granulite dominated crustal contamination pattern is gradually/progressively displaced by a mid-crustal meta-sediment influence during later activity.
- The Hf and Nd isotope compositions of Ruapehu andesites imply a parental magma with significant (>0.5%) source addition of subducted sediment.
- Lower crustal granulites preserved as xenoliths in Ruapehu andesites have Sr, Nd and Hf isotopic compositions that are consistent with derivation from old, altered oceanic crust that has incorporated small amounts of sediment and/or was derived from an originally enriched mantle source.
- Hf and Nd isotopic compositions of the Ruapehu xenoliths suggest they are not important crustal components involved in the evolution of the TVZ basalts, although they are likely to have played a significant role in the evolution of early Ruapehu andesites.
- The similar geochemical properties of Hf and Nd result in broadly linear variations in isotopic compositions during mantle -sediment interactions. This study demonstrates that if at least one end-member in the magmatic system can be firmly identified, extrapolations through volcanic data sets can be used to better constrain compositional variations required for other end-members involved.
- Our results indicate that combined Hf and Nd isotope studies are a potentially powerful means of seeing through processes of crustal contamination and better constraining processes at the slab-wedge interface in continental subduction zones.

## Acknowledgements

Joel Baker and David Ulfbeck are thanked for assistance in the Danish Lithosphere Centre AXIOM MC-ICPMS lab which was funded by the Danish National Research Foundation. TW, JG and RP thank staff of the NZ Department of Conservation, and in particular Dr JR Keys, for long term support of research on Ruapehu Volcano. Nick Mortimer supplied the TVZ basement samples after selection from the PETLAB database. VRT and JG acknowledge funding from Science Foundation Ireland

(SFI) and VRT also from the Swedish Research Council (VR). JPC is grateful for PhD funding by Trinity College in Dublin and an EC Marie Curie mobility scholarship to work in Copenhagen. Simon Barker and three anonymous reviewers are thanked for their comments.

## Appendix A. Supplementary data

Supplementary data to this article can be found online at <http://dx.doi.org/10.1016/j.lithos.2017.04.009>.

## References

- Adams, C.J., Maas, R., 2004. Rb-Sr age and strontium isotopic characterisation of the Torlesse Supergroup in Canterbury, New Zealand, and implications for the status of the Rakaia Terrane. *New Zealand Journal of Geology and Geophysics* 47, 201–217.
- Adams, C.J., Campbell, H.J., Griffin, W.J., 2008. Age and provenance of basement rocks of the Chatham Islands: an outpost of Zealandia. *New Zealand Journal of Geology and Geophysics* 51, 245–259.
- Adams, C.J., Mortimer, N., Campbell, H.J., Griffin, W.L., 2009. Age and isotopic characterisation of metasedimentary rocks from the Torlesse Supergroup and Waipapa Group in the central North Island, New Zealand. *New Zealand Journal of Geology and Geophysics* 52, 149–170.
- Arevalo, R., McDonough, W.F., 2010. Chemical variations and regional diversity observed in MORB. *Chemical Geology* 271:70–85. <http://dx.doi.org/10.1016/j.chemgeo.2009.12.013>.
- Ayres, M., Harris, N., 1997. REE fractionation and Nd-isotope disequilibrium during crustal anatexis: constraints from Himalayan leucogranites. *Chemical Geology* 139:249–269. [http://dx.doi.org/10.1016/s0009-2541\(97\)00038-7](http://dx.doi.org/10.1016/s0009-2541(97)00038-7).
- Barker, S.J., Wilson, C.J.N., Baker, J.A., Millet, M.-A., Rotella, M.D., Wright, I.C., Wysoczanski, R.J., 2013. *Geochemistry and petrogenesis of silicic magmas in the intra-oceanic Kermadec Arc*. *Journal of Petrology* 54, 351–391.
- Barker, S.J., Wilson, C.J.N., Smith, E.G.C., Charlier, B.L.A., Wooden, J.L., Hiess, J., Ireland, T.R., 2014. Post-eruption magmatic reconstruction of Taupo Volcano (New Zealand), as reflected in zircon ages and trace elements. *Journal of Petrology* 55, 1511–1533.
- Barker, S.J., Wilson, C.J.N., Allan, A.S.R., Schipper, C.I., 2015. Fine-scale temporal recovery, reconstruction and evolution of a post-supereruption magma system. *Contributions to Mineralogy and Petrology* 170:5. <http://dx.doi.org/10.1007/s00410-015-1155-2>.
- Beard, R., Davidson, J.P., Turner, S., Macpherson, C.G., Lindsay, J.M., Boyce, A.J., 2014. Assimilation of sediments embedded in the oceanic arc crust: myth or reality? *Earth and Planetary Science Letters* 395:51–60. <http://dx.doi.org/10.1016/j.epsl.2014.03.038>.
- Beard, R., Turner, S., Davidson, J.P., Macpherson, C., Lindsay, J.M., 2015. Seeing through the effects of crustal assimilation to assess the source composition beneath the Southern Lesser Antilles Arc. *Journal of Petrology* 56, 815–844.
- Bibby, H.M., Caldwell, T.G., Davey, F.J., Webb, T.H., 1995. Geophysical evidence on the structure of the Taupo Volcanic zone and its hydrothermal circulation. *Journal of Volcanology and Geothermal Research* 68:29–58. [http://dx.doi.org/10.1016/0377-0273\(95\)00007-h](http://dx.doi.org/10.1016/0377-0273(95)00007-h).
- Bierlein, F.P., Craw, D., 2009. Petrogenetic character and provenance of metabasalts in the aspiring and Torlesse Terranes, South Island, New Zealand: implications for the gold endowment of the Otago Schist? *Chemical Geology* 260:301–315. <http://dx.doi.org/10.1016/j.chemgeo.2009.01.016>.
- Blattner, P., Reid, F., 1982. The origin of lavas and ignimbrites of the Taupo Volcanic Zone, New Zealand, in the light of oxygen isotope data. *Geochimica et Cosmochimica Acta* 46:1417–1429. [http://dx.doi.org/10.1016/0016-7037\(82\)90276-9](http://dx.doi.org/10.1016/0016-7037(82)90276-9).
- Blichert-Toft, J., Agranier, A., Andres, M., Kingsley, R., Schilling, J.G., Albarède, F., 2005. Geochemical segmentation of the Mid-Atlantic Ridge north of Iceland and ridge-hot spot interaction in the North Atlantic. *Geochemistry, Geophysics, Geosystems* 6:27. <http://dx.doi.org/10.1029/2004gc000788>.
- Bouvier, A., Vervoort, J.D., Patchett, P.J., 2008. The Lu-Hf and Sm-Nd isotopic composition of CHUR: constraints from unequilibrated chondrites and implications for the bulk composition of terrestrial planets. *Earth and Planetary Science Letters* 273, 48–57.
- Brown, S.J.A., Smith, R.T., 2004. Crystallisation history and crustal inheritance in a large silicic magma system: Pb-206/U-238 ion probe dating of zircons from the 1.2 Ma Ongatiti ignimbrite, Taupo Volcanic Zone. *Journal of Volcanology and Geothermal Research* 135:247–257. <http://dx.doi.org/10.1016/j.jvolgeores.2004.03.004>.
- Browne, P.R.L., Graham, I.J., Parker, R.J., Wood, C.P., 1992. Subsurface andesite lavas and plutonic rocks in the Rotokawa and Ngatamariki geothermal systems, Taupo Volcanic Zone, New Zealand. *Journal of Volcanology and Geothermal Research* 51:199–215. [http://dx.doi.org/10.1016/0377-0273\(92\)90123-u](http://dx.doi.org/10.1016/0377-0273(92)90123-u).
- Carter, L., Carter, R.M., McCave, I.N., Gamble, J.A., 1996. Regional sediment recycling in the abyssal SW Pacific Ocean. *Geology* 24, 735–738.
- Chadwick, J.P., Troll, V.R., Ginibre, C., Morgan, D., Gertisser, R., Waight, T.E., Davidson, J.P., 2007. Carbonate assimilation at Merapi volcano, Java, Indonesia: insights from crystal isotope stratigraphy. *Journal of Petrology* 48:1793–1812. <http://dx.doi.org/10.1093/petrology/egm038>.
- Chadwick, J.P., Troll, V.R., Waight, T.E., van der Zwan, F.M., Schwarzkopf, L.M., 2013. Petrology and geochemistry of igneous inclusions in recent Merapi deposits: a window into the sub-volcanic plumbing system. *Contributions to Mineralogy and Petrology* 165:259–282. <http://dx.doi.org/10.1007/s00410-012-0808-7>.
- Chambefort, I., Lewis, B., Wilson, C.J.N., Rae, A.J., Coutts, C., Bignall, G., Ireland, T.R., 2014. Stratigraphy and structure of the Ngatamariki geothermal system from new zircon

- U-Pb geochronology: implications for Taupo Volcanic Zone evolution.** *Journal of Volcanology and Geothermal Research* 274, 51–70.
- Charlier, B.L.A., Wilson, C.J.N., Lowenstern, J.B., Blake, S., Van Calsteren, P.W., Davidson, J.P., 2005. Magma generation at a large, hyperactive silicic volcano (Taupo, New Zealand) revealed by U-Th and U-Pb systematics in zircons. *Journal of Petrology* 46:3–32. <http://dx.doi.org/10.1093/petrology/egh060>.
- Charlier, B.L.A., Wilson, C.J.N., Davidson, J.P., 2008. Rapid open-system assembly of a large silicic magma body: time-resolved evidence from cored plagioclase crystals in the Oruanui eruption deposits, New Zealand. *Contributions to Mineralogy and Petrology* 156:799–813. <http://dx.doi.org/10.1007/s00410-008-0316-y>.
- Charlier, B.L.A., Wilson, C.J.N., Mortimer, N., 2010. Evidence from zircon U-Pb age spectra for crustal structure and felsic magma genesis at Taupo volcano, New Zealand. *Geology* 38:915–918. <http://dx.doi.org/10.1130/g31123.1>.
- Chauvel, C., Lewin, E., Carpentier, M., Arndt, N.T., Marini, J.-C., 2008. Role of recycled oceanic basalt and sediment in generating the Hf-Nd mantle array. *Nature Geoscience* 1: 64–67. <http://dx.doi.org/10.1038/ngeo.2007.51>.
- Chen, Y.-X., Gao, P., Zheng, Y.-F., 2015. The anatetic effect on the zircon Hf isotope composition of migmatites and associated granites. *Lithos* 238, 174–184.
- Claeson, D.T., Meurer, W.P., 2004. Fractional crystallization of hydrous basaltic "arc-type" magmas and the formation of amphibole-bearing gabbroic cumulates. *Contributions to Mineralogy and Petrology* 147:288–304. <http://dx.doi.org/10.1007/s00410-003-0536-0>.
- Cole, J.W., 1990. Structural control and origin of volcanism in the Taupo Volcanic Zone, New Zealand. *Bulletin of Volcanology* 52:445–459. <http://dx.doi.org/10.1007/bf00268925>.
- Cole, J.W., Thordarson, T., Burt, R.M., 2000. Magma origin and evolution of White Island (Whakaari) volcano, Bay of Plenty, New Zealand. *Journal of Petrology* 41:867–895. <http://dx.doi.org/10.1093/petrology/41.6.867>.
- Conway, C.E., Townsend, D.B., Leonard, G.S., Wilson, C.J.N., Calvert, A.T., Gamble, J.A., 2015. Lava-ice interaction on a large composite volcano: a case study from Ruapehu, New Zealand. *Bulletin of Volcanology* 77, 21.
- Conway, C.E., Leonard, G.S., Townsend, D.B., Calvert, A.T., CJN, Wilson, Gamble, J.A., Eaves, S.R., 2016. A high resolution 40Ar/39Ar lava chronology and construction history for Ruapehu Volcano, New Zealand. *Journal of Volcanology and Geothermal Research* 327, 152–179.
- Dahren, B., Troll, V.R., Andersson, U.B., Chadwick, J.P., Gardner, M.F., Jaxybulatov, K., Koukalov, I., 2012. Magma plumbing beneath Anak Krakatau volcano, Indonesia: evidence for multiple magma storage regions. *Contributions to Mineralogy and Petrology* 163:631–651. <http://dx.doi.org/10.1007/s00410-011-0690-8>.
- Darby, D.J., Meertens, C.M., 1995. Terrestrial and GPS measurements of the deformation across the Taupo back-arc and Hikurangi fore-arc regions in New Zealand. *Journal of Geophysical Research - Solid Earth* 100 (B5):8221–8232. <http://dx.doi.org/10.1029/94jb03265>.
- Davidson, J., Wilson, M., 2011. Differentiation and source processes at Mt Pelee and the Quill; active volcanoes in the Lesser Antilles arc. *Journal of Petrology* 52:1493–1531. <http://dx.doi.org/10.1093/petrology/egg095>.
- Davidson, J.P., Hora, J.M., Garrison, J.M., Dungan, M.A., 2005. Crustal forensics in arc magmas. *Journal of Volcanology and Geothermal Research* 140:157–170. <http://dx.doi.org/10.1016/j.jvolgeores.2004.07.019>.
- Davidson, J.P., Morgan, D.J., Charlier, B.L.A., Harlou, R., Hora, J.M., 2007. Microsampling and isotopic analysis of igneous rocks: implications for the study of magmatic systems. *Annual Review of Earth and Planetary Sciences* 35, 273–311.
- Davies, G.R., Tommasini, S., 2000. Isotopic disequilibrium during rapid crustal anatexis: implications for petrogenetic studies of magmatic processes. *Chemical Geology* 162:169–191. [http://dx.doi.org/10.1016/S0009-2541\(99\)00123-0](http://dx.doi.org/10.1016/S0009-2541(99)00123-0).
- De Paolo, D.J., 1981. Trace element and isotopic effects of combined wallrock assimilation and fractional crystallization. *Earth and Planetary Science Letters* 53:189–202. [http://dx.doi.org/10.1016/0012-821x\(81\)90153-9](http://dx.doi.org/10.1016/0012-821x(81)90153-9).
- Deering, C.D., Cole, J.W., Vogel, T.A., 2008. A rhyolite compositional continuum governed by lower crustal source conditions in the Taupo Volcanic Zone, New Zealand. *Journal of Petrology* 49:2245–2276. <http://dx.doi.org/10.1093/petrology/egn067>.
- Duggen, S., Hoernle, K., Kluegel, A., Geldmacher, J., Thirlwall, M., Hauff, F., Lowry, D., Oates, N., 2008. Geochemical zonation of the Miocene Alboran Basin volcano (westernmost Mediterranean): geodynamic implications. *Contributions to Mineralogy and Petrology* 156:577–593. <http://dx.doi.org/10.1007/s00410-008-0302-4>.
- Elliott, T., Plank, T., Zindler, A., White, W., Bourdon, B., 1997. Element transport from slab to volcanic front at the Mariania arc. *Journal of Geophysical Research - Solid Earth* 102 (B7):14991–15019. <http://dx.doi.org/10.1029/97jb00788>.
- Gamble, J.A., Smith, I.E.M., Graham, I.J., Kokelaar, B.P., Cole, J.W., Houghton, B.F., Wilson, C.J.N., 1990. The petrology, phase-relations and tectonic setting of basalts from the Taupo Volcanic Zone, New Zealand and the Kermadec Island Arc-Havre Trough, SW Pacific. *Journal of Volcanology and Geothermal Research* 43:253–270. [http://dx.doi.org/10.1016/0377-0273\(90\)90055-k](http://dx.doi.org/10.1016/0377-0273(90)90055-k).
- Gamble, J.A., Smith, I.E.M., McCulloch, M.T., Graham, I.J., Kokelaar, B.P., 1993a. The geochemistry and petrogenesis of basalts from the Taupo Volcanic Zone and Kermadec Island arc, SW Pacific. *Journal of Volcanology and Geothermal Research* 54:265–290. [http://dx.doi.org/10.1016/0377-0273\(93\)90067-2](http://dx.doi.org/10.1016/0377-0273(93)90067-2).
- Gamble, J.A., Wright, I.C., Baker, J.A., 1993b. Seafloor geology and petrology in the oceanic to continental transition zone of the Kermadec-Havre-Taupo Volcanic Zone arc system, New Zealand. *New Zealand Journal of Geology and Geophysics* 36, 417–435.
- Gamble, J., Wright, I.C., Woodhead, J., McCulloch, M.T., 1994. Arc and back-arc geochemistry in the southern Kermadec-Ngatoro Basin and offshore Taupo Volcanic Zone, SW Pacific. In: Smellie, J.L. (Ed.), *Volcanism Associated with Extension at Consuming Plate Margins*. Geological Society of London Special Publications vol. 81, pp. 193–212.
- Gamble, J., Woodhead, J., Wright, I., Smith, I., 1996. Basalt and sediment geochemistry and magma petrogenesis in a transect from oceanic island arc to rifted continental margin arc: the Kermadec Hikurangi Margin, SW Pacific. *Journal of Petrology* 37:1523–1546. <http://dx.doi.org/10.1093/petrology/37.6.1523>.
- Gamble, J.A., Wood, C.P., Price, R.C., Smith, I.E.M., Stewart, R.B., Waught, T., 1999. A fifty year perspective of magmatic evolution on Ruapehu Volcano, New Zealand: verification of open system behaviour in an arc volcano. *Earth and Planetary Science Letters* 170:301–314. [http://dx.doi.org/10.1016/s0012-821x\(99\)00106-5](http://dx.doi.org/10.1016/s0012-821x(99)00106-5).
- Geldmacher, J., Hoernle, K., Hanan, B.B., Blichert-Toft, J., Hauff, F., Gill, J.B., Schmincke, H.U., 2011. Hafnium isotopic variations in East Atlantic intraplate volcanism. *Contributions to Mineralogy and Petrology* 162:21–36. <http://dx.doi.org/10.1007/s00410-010-0580-5>.
- Graham, I.J., Hackett, W.R., 1987. Petrology of calc-alkaline lavas from Ruapehu volcano and related vents, Taupo Volcanic Zone, New Zealand. *Journal of Petrology* 28, 531–567.
- Graham, I.J., Grapes, R.H., Kifle, K., 1988. Buchitic metagreywacke xenoliths from Mount Ngauruhoe, Taupo Volcanic Zone, New Zealand. *Journal of Volcanology and Geothermal Research* 35:205–216. [http://dx.doi.org/10.1016/0377-0273\(88\)90017-0](http://dx.doi.org/10.1016/0377-0273(88)90017-0).
- Graham, I.J., Blattner, P., McCulloch, M.T., 1990. Meta-igneous granulite xenoliths from Mount Ruapehu, New Zealand - fragments of altered oceanic crust. *Contributions to Mineralogy and Petrology* 105:650–661. <http://dx.doi.org/10.1007/bf00306531>.
- Graham, I.J., Gulson, B.L., Hednequist, J.W., Mizon, K., 1992. Petrogenesis of late Cenozoic volcanic rocks from the Taupo Volcanic zone, New Zealand, in the light of new lead isotope data. *Geochimica et Cosmochimica Acta* 56:2797–2819. [http://dx.doi.org/10.1016/0016-7037\(92\)90360-u](http://dx.doi.org/10.1016/0016-7037(92)90360-u).
- Graham, I.J., Cole, J.W., Briggs, R.M., Gamble, J.A., Smith, I.E.M., 1995. Petrology and petrogenesis of volcanic rocks from the Taupo Volcanic Zone - a review. *Journal of Volcanology and Geothermal Research* 68:59–87. [http://dx.doi.org/10.1016/0377-0273\(95\)00008-i](http://dx.doi.org/10.1016/0377-0273(95)00008-i).
- Handley, H.K., Macpherson, C.G., Davidson, J.P., Berlo, K., Lowry, D., 2007. Constraining fluid and sediment contributions to subduction-related magmatism in Indonesia: Ijen Volcanic Complex. *Journal of Petrology* 48:1155–1183. <http://dx.doi.org/10.1093/petrology/egm013>.
- Handley, H.K., Turner, S., Macpherson, C.G., Gertisser, R., Davidson, J.P., 2011. Hf-Nd isotope and trace element constraints on subduction inputs at island arcs: limitations of Hf anomalies as sediment input indicators. *Earth and Planetary Science Letters* 304:212–223. <http://dx.doi.org/10.1016/j.epsl.2011.01.034>.
- Hiess, J., Cole, J.W., Spinks, K.D., 2007. Influence of the crust and crustal structure on the location and composition of high-alumina basalts of the Taupo Volcanic Zone, New Zealand. *New Zealand Journal of Geology and Geophysics* 50, 327–342.
- Hobden, B.J., Houghton, B.F., Nairn, I.A., 2002. Growth of a young, frequently active composite cone: Ngauruhoe volcano, New Zealand. *Bulletin of Volcanology* 64:392–409. <http://dx.doi.org/10.1007/s0445-002-0216-3>.
- Hochstein, M.P., Smith, I.E.M., Regenauerlieb, K., Ehara, S., 1993. Geochemistry and heat-transfer processes in Quaternary rhyolitic systems of the Taupo Volcanic Zone, New Zealand. *Tectonophysics* 223:213–235. [http://dx.doi.org/10.1016/0040-1951\(93\)90139-b](http://dx.doi.org/10.1016/0040-1951(93)90139-b).
- Hofmann, A.W., 2003. Sampling mantle heterogeneity through oceanic basalts: isotopes and trace elements. In: Holland, H., Turekian, K. (Eds.), *Treatise on Geochemistry* vol. 2, pp. 1–44.
- Kent, A.J.R., Darr, C., Koleszar, A.M., Salisbury, M.J., Cooper, K.M., 2010. Preferential eruption of andesitic magmas through recharge filtering. *Nature Geoscience* 3:631–636. <http://dx.doi.org/10.1038/ngeo924>.
- Knesel, K.M., Davidson, J.P., 1996. Isotopic disequilibrium during melting of granite and implications for crustal contamination of magmas. *Geology* 24:243–246. [http://dx.doi.org/10.1130/0091-7613\(1996\)024-0243:iddmog-2.3;2](http://dx.doi.org/10.1130/0091-7613(1996)024-0243:iddmog-2.3;2).
- Langmuir, C.H., Vocke, R.D., Hanson, G.N., Hart, S.R., 1978. General mixing equation with applications to Icelandic basalts. *Earth and Planetary Science Letters* 37:380–392. [http://dx.doi.org/10.1016/0012-821x\(78\)90053-5](http://dx.doi.org/10.1016/0012-821x(78)90053-5).
- Macpherson, C.G., Gamble, J.A., Matthey, D.P., 1998. Oxygen isotope geochemistry of lavas from an oceanic to continental arc transition, Kermadec-Hikurangi margin, SW Pacific. *Earth and Planetary Science Letters* 160, 609–621.
- Martindale, M., Skora, S., Pickles, J., Elliott, T., Blundy, J., Avanzinelli, R., 2013. High pressure phase relations of subducted volcanioclastic sediments from the west Pacific and their implications for the geochemistry of Mariana arc magmas. *Chemical Geology* 342: 94–109. <http://dx.doi.org/10.1016/j.chemgeo.2013.01.015>.
- McCormack, K.D., Gee, M.A.M., McNaughton, N.J., Smith, R., Fletcher, I.R., 2009. U-Pb dating of magmatic and xenocryst zircons from Mangakino ignimbrites and their correlation with detrital zircons from the Torlesse metasediments, Taupo Volcanic Zone, New Zealand. *Journal of Volcanology and Geothermal Research* 183:97–111. <http://dx.doi.org/10.1016/j.jvolgeores.2009.03.005>.
- McCulloch, M.T., Kyser, T.K., Woodhead, J.D., Kinsley, L., 1994. Pb-Sr-Nd-O isotopic constraints on the origin of rhyolites from the Taupo Volcanic Zone of New Zealand - evidence for assimilation followed by fractionation from basalt. *Contributions to Mineralogy and Petrology* 115:303–312. <http://dx.doi.org/10.1007/bf00310769>.
- Meade, F.C., Troll, V.R., Ellam, R.M., Freda, C., Font, L., Donaldson, C.H., Klonowska, I., 2014. Bimodal magmatism produced by progressively inhibited crustal assimilation. *Nature Communications* 5. <http://dx.doi.org/10.1038/ncomms5199>.
- Mortimer, N., 2004. New Zealand's geological foundations. *Gondwana Research* 7: 261–272. [http://dx.doi.org/10.1016/s1342-937x\(05\)70324-5](http://dx.doi.org/10.1016/s1342-937x(05)70324-5).
- Mortimer, N., Tulloch, A.J., Ireland, T.R., 1997. Basement geology of Taranki and Wanganui Basins, New Zealand. *New Zealand Journal of Geology and Geophysics* 40, 223–236.
- Nakagawa, M., Wada, K., Wood, C.P., 2002. Mixed magmas, mush chambers and eruption triggers: evidence from zoned clinopyroxene phenocrysts in andesitic scoria from the 1995 eruptions of Ruapehu volcano, New Zealand. *Journal of Petrology* 43: 2279–2303. <http://dx.doi.org/10.1093/petrology/43.12.2279>.
- Patchett, P.J., White, W.M., Feldmann, H., Kielinczuk, S., Hofmann, A.W., 1984. Hafnium rare earth element fractionation in the sedimentary system and crustal recycling into the

- Earth's mantle. *Earth and Planetary Science Letters* 69:365–378. [http://dx.doi.org/10.1016/0012-821x\(84\)90195-x](http://dx.doi.org/10.1016/0012-821x(84)90195-x).
- Pearce, J.A., Kempton, P.D., Nowell, G.M., Noble, S.R., 1999. Hf-Nd element and isotope perspective on the nature and provenance of mantle and subduction components in Western Pacific arc-basin systems. *Journal of Petrology* 40:1579–1611. <http://dx.doi.org/10.1093/petrology/40.11.1579>.
- Pearce, J.A., Kempton, P.D., Gill, J.B., 2007. Hf-Nd evidence for the origin and distribution of mantle domains in the SW Pacific. *Earth and Planetary Science Letters* 260:98–114. <http://dx.doi.org/10.1016/j.epsl.2007.05.023>.
- Plank, T., Langmuir, C.H., 1993. Tracing trace elements from sediment input to volcanic output at subduction zones. *Nature* 362:739–743. <http://dx.doi.org/10.1038/362739a0>.
- Plank, T., Langmuir, C.H., 1998. The chemical composition of subducting sediment and its consequences for the crust and mantle. *Chemical Geology* 145:325–394. [http://dx.doi.org/10.1016/s0009-2541\(97\)00150-2](http://dx.doi.org/10.1016/s0009-2541(97)00150-2).
- Price, R.C., Gamble, J.A., Smith, I.E.M., Stewart, R.B., Eggins, S., Wright, I.C., 2005. An integrated model for the temporal evolution of andesites and rhyolites and crustal development in New Zealand's North Island. *Journal of Volcanology and Geothermal Research* 140:1–24. <http://dx.doi.org/10.1016/j.jvolgeores.2004.07.013>.
- Price, R.C., George, R., Gamble, J.A., Turner, S., Smith, I.E.M., Cook, C., Hobden, B., Dosseto, A., 2007. U-Th-Ra fractionation during crustal-level andesite formation at Ruapehu volcano, New Zealand. *Chemical Geology* 244:437–451. <http://dx.doi.org/10.1016/j.chemgeo.2007.07.001>.
- Price, R.C., Turner, S., Cook, C., Hobden, B., Smith, I.E.M., Gamble, J.A., Handley, H., Maas, R., Mobis, A., 2010. Crustal and mantle influences and U-Th-Ra disequilibrium in anandesitic lavas of Ngauruhoe volcano, New Zealand. *Chemical Geology* 277:355–373. <http://dx.doi.org/10.1016/j.chemgeo.2010.08.021>.
- Price, R.C., Gamble, J.A., Smith, I.E.M., Maas, R., Waight, T., Stewart, R.B., Woodhead, J., 2012. The anatomy of an andesite volcano: a time-stratigraphic study of andesite oogenesis and crustal evolution at Ruapehu Volcano, New Zealand. *Journal of Petrology* 53:2139–2189. <http://dx.doi.org/10.1093/petrology/egs050>.
- Price, R.C., Mortimer, N., Smith, I.E.M., Maas, R., 2015. Whole-rock geochemical reference data for Torlesse and Waipapa terranes, North Island, New Zealand. *New Zealand Journal of Geology and Geophysics* 58:213–228. <http://dx.doi.org/10.1080/00288306.2015.1026832>.
- Reubi, O., Blundy, J., 2009. A dearth of intermediate melts at subduction zone volcanoes and the petrogenesis of arc andesites. *Nature* 461:1269–1273. <http://dx.doi.org/10.1038/nature08510>.
- Rooney, T.O., Deering, C.D., 2013. Conditions of melt generation beneath the Taupo Volcanic Zone: the influence of heterogeneous mantle inputs on large-volume silicic systems. *Geology* 42:3–6. <http://dx.doi.org/10.1130/g34868.1>.
- Rudnick, R.L., Gao, S., 2003. Composition of the continental crust. In: Holland, H., Turekian, K. (Eds.), *Treatise on Geochemistry* vol. 3. Elsevier, pp. 1–64.
- Saltert, V.J.M., Stracke, A., 2004. Composition of the depleted mantle. *Geochemistry, Geophysics, Geosystems* 5, Q05004. <http://dx.doi.org/10.1029/2003GC000597>.
- Scott, J.M., Waight, T.E., van der Meer, Q.H.A., Palin, J.M., Cooper, A.F., Münker, C., 2014. Metasomatised ancient lithospheric mantle beneath the young Zealandia microcontinent and its role in HIMU-like intraplate magmatism. *Geochemistry, Geophysics, Geosystems* 15 (9):3477–3501. <http://dx.doi.org/10.1002/2014gc005300>.
- Skora, S., Blundy, J., 2010. High-pressure hydrous phase relations of radiolarian clay and implications for the involvement of subducted sediment in arc magmatism. *Journal of Petrology* 51:2211–2243. <http://dx.doi.org/10.1093/petrology/eqq054>.
- Skora, S., Blundy, J., 2012. Monazite solubility in hydrous silicic melts at high pressure conditions relevant to subduction zone metamorphism. *Earth and Planetary Science Letters* 321:104–114. <http://dx.doi.org/10.1016/j.epsl.2012.01.002>.
- Smith, I.E.M., Price, R.C., 2006. The Tonga-Kermadec arc and Havre-Lau backarc system: their role in the development of tectonic and magmatic models for the western Pacific. *Journal of Volcanology and Geothermal Research* 156, 315–331.
- Smith, I.E.M., Stewart, R.B., Price, R.C., 2003. The petrology of a large intra-oceanic silicic eruption: the Sandy Bay Tephra, Kermadec Arc, Southwest Pacific. *Journal of Volcanology and Geothermal Research* 124:173–194. [http://dx.doi.org/10.1016/s0377-0273\(03\)00040-4](http://dx.doi.org/10.1016/s0377-0273(03)00040-4).
- Smith, I.E.M., Stewart, R.B., Price, R.C., Worthington, T.J., 2010. Are arc-type rocks the products of magma crystallisation? Observations from a simple oceanic arc volcano: Raoul Island, Kermadec Arc, SW Pacific. *Journal of Volcanology and Geothermal Research* 190:219–234. <http://dx.doi.org/10.1016/j.jvolgeores.2009.05.006>.
- Stern, T.A., 1987. Asymmetric back-arc spreading, heat-flux and structure associated with the central volcanic region of New Zealand. *Earth and Planetary Science Letters* 85: 265–276. [http://dx.doi.org/10.1016/0012-821x\(87\)90037-9](http://dx.doi.org/10.1016/0012-821x(87)90037-9).
- Stern, T., Stratford, W., Seward, A., Henderson, M., Savage, M., Smith, E., Benson, A., Greve, S., Salmon, M., 2010. Crust-mantle structure of the central North Island, New Zealand, based on seismological observations. *Journal of Volcanology and Geothermal Research* 190:58–74. <http://dx.doi.org/10.1016/j.jvolgeores.2009.11.017>.
- Stracke, A., Snow, J.E., Hellebrand, E., von der Handt, A., Bourdon, B., Birbaum, K., Gunther, D., 2011. Abyssal peridotite Hf isotopes identify extreme mantle depletion. *Earth and Planetary Science Letters* 308:359–368. <http://dx.doi.org/10.1016/j.epsl.2011.06.012>.
- Todd, E., Gill, J.B., Wysockanski, R.J., Handler, M.R., Wright, I.C., Gamble, J.A., 2010. Sources of constructional cross-chain volcanism in the southern Havre Trough: new insights from HFSE and REE concentration and isotope systematics. *Geochemistry, Geophysics, Geosystems* 11:31. <http://dx.doi.org/10.1029/2009gc002888>.
- Todd, E., Gill, J.B., Wysockanski, R.J., Hergt, J., Wright, I.C., Leybourne, M.I., Mortimer, N., 2011. Hf isotopic evidence for small-scale heterogeneity in the mode of mantle wedge enrichment: Southern Havre Trough and South Fiji Basin back arcs. *Geochemistry, Geophysics, Geosystems* 12:34. <http://dx.doi.org/10.1029/2011gc003683>.
- Troll, V.R., Deegan, F.M., Jolis, E.M., Harris, C., Chadwick, J.P., Gertisser, R., Schwarzkopf, L.M., Borisova, A.Y., Bindeman, I.N., Sumarti, S., Preece, K., 2013. Magmatic differentiation processes at Merapi Volcano: inclusion petrology and oxygen isotopes. *Journal of Volcanology and Geothermal Research* 261:38–49. <http://dx.doi.org/10.1016/j.jvolgeores.2012.11.001>.
- Turner, S., Handler, M., Bindeman, I., Suzuki, K., 2009. New insights into the origin of O-Hf-O isotope signatures in arc lavas from Tonga-Kermadec. *Chemical Geology* 266: 187–193. <http://dx.doi.org/10.1016/j.chemgeo.2009.05.027>.
- Ulfbeck, D., Baker, J., Waight, T., Krogstad, E., 2003. Rapid sample digestion by fusion and chemical separation of Hf for isotopic analysis by MC-ICPMS. *Talanta* 59:365–373. [http://dx.doi.org/10.1016/s0039-9140\(02\)00525-8](http://dx.doi.org/10.1016/s0039-9140(02)00525-8).
- Vervoort, J.D., Patchett, P.J., Blachert-Toft, J., Albarède, F., 1999. Relationships between Lu-Hf and Sm-Nd isotopic systems in the global sedimentary system. *Earth and Planetary Science Letters* 168:79–99. [http://dx.doi.org/10.1016/s0012-821x\(99\)00047-3](http://dx.doi.org/10.1016/s0012-821x(99)00047-3).
- Waight, T.E., Lesher, C.E., 2010. Pb isotopes during crustal melting and magma mingling – a cautionary tale from the Miki Fjord macrodike, central east Greenland. *Lithos* 118: 191–201. <http://dx.doi.org/10.1016/j.lithos.2010.04.012>.
- Waight, T.E., Price, R.C., Stewart, R.B., Smith, I.E.M., Gamble, J., 1999. Stratigraphy and geochemistry of the Tuoro area, with implications for andesite petrogenesis at Mt Ruapehu, Taupo Volcanic Zone, New Zealand. *New Zealand Journal of Geology and Geophysics* 42, 513–532.
- Wilson, C.J.N., Rowland, J.V., 2016. The volcanic, magmatic and tectonic setting of the Taupo Volcanic Zone, New Zealand, reviews from a geothermal perspective. *Geothermics* 59, 168–187.
- Wilson, C.J.N., Houghton, B.F., McWilliams, M.O., Lanphere, M.A., Weaver, S.D., Briggs, R.M., 1995. Volcanic and structural evolution of Taupo Volcanic Zone, New Zealand – a review. *Journal of Volcanology and Geothermal Research* 68:1–28. [http://dx.doi.org/10.1016/0377-0273\(95\)00006-g](http://dx.doi.org/10.1016/0377-0273(95)00006-g).
- Woodhead, J.D., Hergt, J.M., Davidson, J.P., Eggins, S.M., 2001. Hafnium isotope evidence for 'conservative' element mobility during subduction zone processes. *Earth and Planetary Science Letters* 192:331–346. [http://dx.doi.org/10.1016/s0012-821x\(01\)00453-8](http://dx.doi.org/10.1016/s0012-821x(01)00453-8).
- Woodhead, J., Hergt, J., Pearce, J., Hergt, J., Vervoort, J., 2012. Hf-Nd isotope variation in Mariana Trough basalts: the importance of "ambient mantle" in the interpretation of subduction zone magmas. *Geology* 40:539–542. <http://dx.doi.org/10.1130/g32963.1>.
- Workman, R.K., Hart, S.R., 2005. Major and trace element composition of the depleted MORB mantle (DMM). *Earth and Planetary Science Letters* 231:53–72. <http://dx.doi.org/10.1016/j.epsl.2004.12.005>.
- Wysockanski, R.J., Todd, E., Wright, I.C., Leybourne, M.I., Hergt, J.M., Adam, C., Mackay, K., 2010. Backarc rifting, constructional volcanism and nascent disorganized spreading in the southern Havre Trough backarc rifts (SW Pacific). *Journal of Volcanology and Geothermal Research* 190:39–57. <http://dx.doi.org/10.1016/j.jvolgeores.2009.04.004>.
- Yogodzinski, G.M., Vervoort, J.D., Brown, S.T., Gerseny, M., 2010. Subduction controls of Hf and Nd isotopes in lavas of the Aleutian island arc. *Earth and Planetary Science Letters* 300:226–238. <http://dx.doi.org/10.1016/j.epsl.2010.09.035>.